Supplementary Table E1. Expression profiles of hypoxia-inducible factor-1α–inducible genes in cells treated with NR-101[a]

Gene symbol	Gene name	UT-7/TPO	$CD34^+$
Angiogenesis			
VEGFA	vascular endothelial growth factor A	↑	↑
SERPINE1	serpin peptidase inhibitor	↑	ND
Vasomotor control			
NOS2A	nitric oxide synthase 2A	↑	ND
EDN1	endothelin 1	↑	ND
Erythropoiesis			
EPO	erythropoietin	→	ND
EPOR	erythropoietin receptor	↓	ND
TFRC	transferrin receptor	↑	ND
Glycolysis			
ALDOA	aldolase A, fructose-bisphosphate	↑	ND
PFKL	phosphofructokinase, liver	→	ND
PKM2	pyruvate kinase, muscle	→	ND
ENO1	enolase 1	↑	ND
HK1	hexokinase 1	→	ND
HK2	hexokinase 2	↑	ND
LDHA	lactate dehydrogenase A	↑	ND
PGK1	phosphoglycerate kinase 1	→	ND
Glucose transport			
SLC2A1	solute carrier family 2, number 1	↑	ND
SLC2A3	solute carrier family 2, number 3	↑	↑
Others			
HIF1A	hypoxia-inducible factor 1 α	→	ND
P4HA1	procollagen-proline, α 1	↑	↑
CDKN1A (p21)	cyclin-dependent kinase inhibitor 1A	↑	↑
PIM1	pim-1 oncogene	↑	↑
CXCL12	chemokine (C-X-C motif) ligand 12	↑	↑

↑ = upregulated; ↓ = downregulated; → = unchanged; ND = not determined.
[a]Quantitative polymerase chain reaction.

Brief report

Definitive proof for direct reprogramming of hematopoietic cells to pluripotency

*Motohito Okabe,[1] *Makoto Otsu,[1] Dong Hyuck Ahn,[1] Toshihiro Kobayashi,[1] Yohei Morita,[1] Yukiko Wakiyama,[2] Masafumi Onodera,[3] Koji Eto,[1] Hideo Ema,[1] and Hiromitsu Nakauchi[1,2]

[1]Division of Stem Cell Therapy, Center for Stem Cell and Regenerative Medicine, Institute of Medical Science, University of Tokyo, Tokyo; [2]Japan Science and Technology Agency, Exploratory Research for Advanced Technology, Nakauchi Stem Cell and Organ Regeneration Project, Tokyo; and [3]Department of Genetics, National Research Institute for Child Health and Development, Tokyo, Japan

Generation of induced pluripotent stem cells (iPSCs) generally uses fibroblastic cells, but other cell sources may prove useful in both research and clinical settings. Although proof of cellular origin requires genetic-marker identification in both target cells and established iPSCs, somatic cells other than mature lymphocytes mostly lack such markers. Here we show definitive proof of direct reprogramming of murine hematopoietic cells with no rearranged genes. Using iPSC factor transduction, we successfully derived iPSCs from bone marrow progenitor cells obtained from a mouse whose hematopoiesis was reconstituted from a single congenic hematopoietic stem cell. Established clones were demonstrated to be genetically identical to the transplanted single hematopoietic stem cell, thus proving their cellular origin. These hematopoietic cell–derived iPSCs showed typical characteristics of iPSCs, including the ability to contribute to chimerism in mice. These results will prompt further use of hematopoietic cells for iPSC generation while enabling definitive studies to test how cellular sources influence characteristics of descendant iPSCs. (Blood. 2009; 114:1764-1767)

Introduction

Development of induced pluripotent stem cell (iPSC) technology has enabled generation of disease-specific pluripotent stem cells from the patient.[1] A typical method uses virus-mediated transfer of defined factors into fibroblastic cells[2-4] or marrow-derived mesenchymal cells.[1,5] Some other tissues are also reported as sources for iPSC generation, including murine hepatocytes and gastric epithelial cells,[6] human keratinocytes,[7] and very recently, human blood.[8] As the variability of cellular sources becomes greater, it is attractive to address an interesting question: is each iPSC clone derived from distinct sources unique in its characteristics? Although definitive proof of iPSC cellular origin requires genetic markers, as most somatic cells (except mature lymphocytes) lack such markers, no formal data have shown reprogramming of hematopoietic cells, aside from one study that used immunoglobulin genes as markers.[9] Here, we demonstrate definitive proof for a direct reprogramming to pluripotency of primary marrow hematopoietic cells with no gene rearrangement.

Methods

Mice

Animal experiments were performed with approval of the Institutional Animal Care and Use Committee of the Institute of Medical Science, University of Tokyo.

Generation of iPSCs from murine bone marrow progenitor cells

Lineage marker–negative (Lin^-) c-Kit^+ (Kit^+) cells were enriched using immunomagnetic beads. pMXs vectors[10] encoding iPSC genes are described.[1] Concentrated vesicular stomatitis virus-G–retroviral supernatant was prepared using reported procedures.[11-13] 293GP and 293GPG cells were kind gifts from Dr R. C. Mulligan (Children's Hospital Boston, Harvard Medical School, Boston, MA).[14] Detailed procedures are described in the text and supplemental data (available on the *Blood* website; see the Supplemental Materials link at the top of the online article).

In vitro and in vivo assessment of iPSCs

Characteristics of iPSCs were assessed following reported procedures.[1] Primer sequences are shown in supplemental Table 1. Immunoglobulin heavy chain gene rearrangement was analyzed following described methods.[15,16] A single-base difference within *Cd45* exon 25 was analyzed as reported.[17]

Results and discussion

To prove the cellular origin of iPSC clones formally, use of definitive genetic markers is necessary, as with reported reprogramming of mature B cells[9] and pancreatic beta cells.[18] Even if iPSCs are generated from hematopoietic stem/progenitor cells (HSPCs), nearly 100% positive for the hematopoietic marker CD45, one might argue, in light of reported generation of iPSCs from marrow stromal cells,[1,5] that a small number of nonhematopoietic cells had been reprogrammed. However, no such suitable marker exists for hematopoietic cells (excepting rearranged immunoreceptor genes in mature lymphocytes). We therefore exploited a prominent characteristic of the hematopoietic system: transplantation of a single hematopoietic stem cell (HSC) can reconstitute host hematopoiesis.[19]

Submitted February 4, 2009; accepted May 11, 2009. Prepublished online as *Blood* First Edition paper, June 29, 2009; DOI 10.1182/blood-2009-02-203695.

*M. Okabe and M. Otsu contributed equally to this work.

The online version of this article contains a data supplement.

The publication costs of this article were defrayed in part by page charge payment. Therefore, and solely to indicate this fact, this article is hereby marked "advertisement" in accordance with 18 USC section 1734.

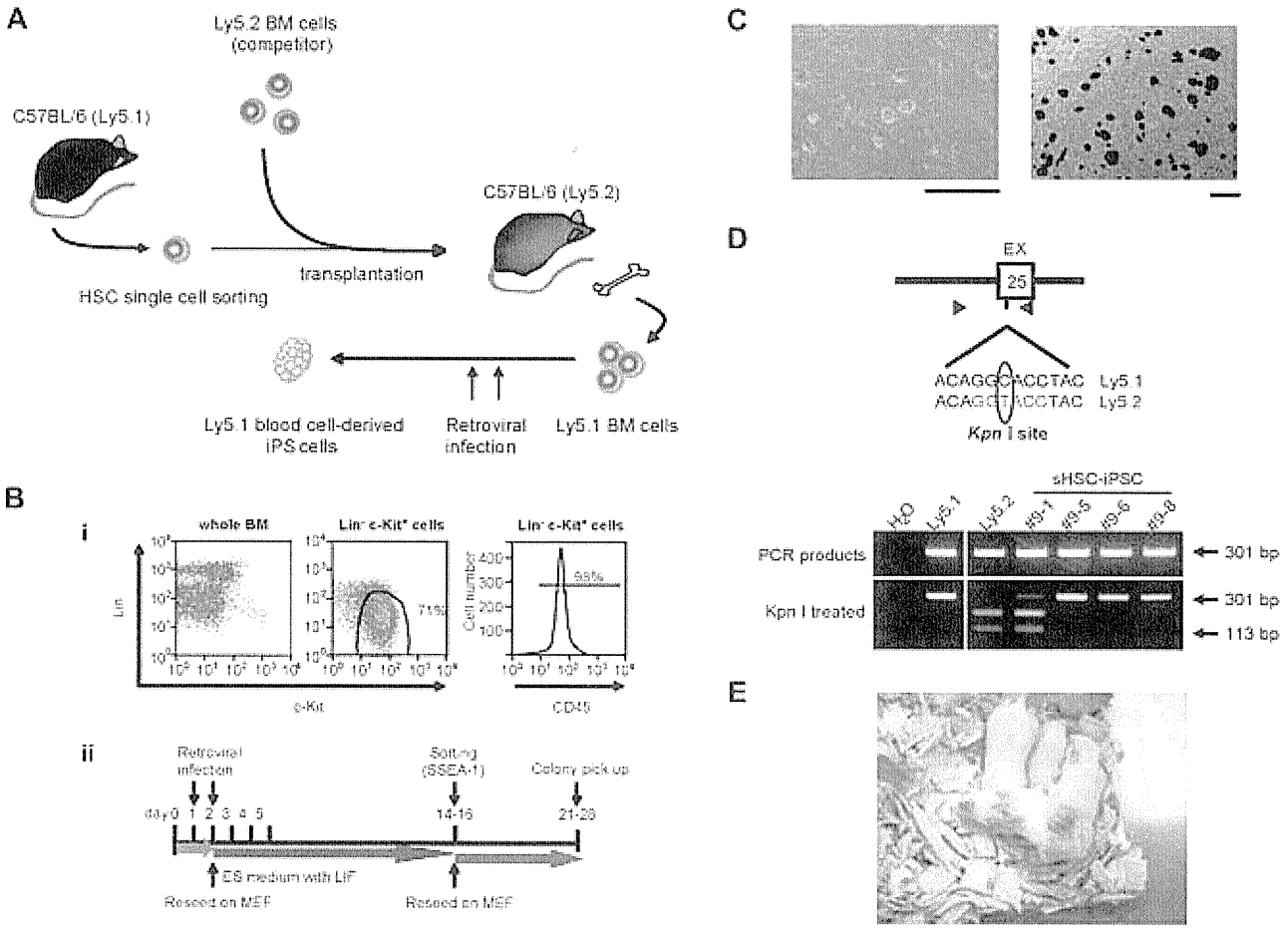

Figure 1. Proof of iPSC induction from hematopoietic cells in a single-HSC transplantation model. (A) Schematic representation of the experimental procedure. Single $CD150^+CD34^{-/low}$ KSL cells obtained from B6 Ly5.1 mice were transplanted into lethally irradiated B6 Ly5.2 mice together with BM cells from B6 Ly5.2 mice. BM HSPCs were obtained from a recipient mouse that showed long-term (~ 10 months) stable Ly5.1 chimerism (~ 80%), enriched for $Ly5.1^+$ cells, and subjected to iPSC generation. (B) A schematic diagram of iPSC generation from BM HSPCs. (i) Lineage markers (Lin) versus c-Kit plots are shown for cells either before (whole BM) or after ($Lin^-c\text{-}Kit^+$) purification. Note that purified HSPCs are 98% CD45-positive. (ii) A schematic diagram of iPSC generation from BM HSPCs. (C) Typical ES cell–like appearance of sHSC-iPS cell colonies (left) with high ALP activities (right). Bars represent 100 μm. (D) Determination of the cellular origin of sHSC-iPSC clones. (Top panel) Scheme of the polymerase chain reaction (PCR)–based method used, using a single-base polymorphism at *Cd45* exon (EX) 25. Black triangles represent primer positions. Ly5.1 and Ly5.2 strains differ by a single base in EX 25, as shown in the presented 12-bp sequences from within the 301-bp amplicons. Treatment with the restriction enzyme *KpnI* leaves the $Ly5.1^+$ cell–derived amplicon undigested, whereas it generates 2 smaller fragments (113 bp + 188 bp) from the $Ly5.2^+$ counterpart. The gel images (bottom panel) indicate that, of 4 sHSC-iPSC clones, 1 (no. 9-1) is of $Ly5.2^+$ cell origin, whereas 3 (nos. 9-5, -6, and -8) are derived from $Ly5.1^+$ cells that originated from a single $Ly5.1^+$ HSC. A vertical line has been inserted to indicate a repositioned gel lane. (E) Chimeric mice obtained by implantation of sHSC-iPSC clone 9-5 into ICR host blastocysts.

Figure 1A depicts our experimental design. We attempted iPSC generation from marrow HSPCs harvested long-term (~ 10 months) after reconstitution from a single HSC of C57BL6 (B6) Ly 5.1 origin. We used concentrated vesicular stomatitis virus-G–pseudotyped retroviruses,[14] as we had succeeded in their efficient transduction into murine HSPCs.[12,13] We purified from bone marrow (BM) of a reconstituted mouse (B6 Ly5.2) Lin^-Kit^+ cells, a HSPC population, with approximately 98% of cells expressing CD45 (Figure 1B). We then transduced these cells with a cocktail of retroviral vectors harboring each of the iPSC factor genes *Oct4*, *Sox2*, *Klf4*, and *c-Myc*, transferred onto mouse embryonic fibroblast cells, and maintained in the presence of leukemia inhibitory factor until cell sorting (Figure 1B). Visible iPSC-like colonies appeared on approximately days 9 to 11 among a majority of hematopoietic cells that remained nonreprogrammed; these colonies then grew steadily (supplemental Figure 1A). To enrich iPSC candidates, we sorted the cells expressing SSEA-1 on approximately days 14 to 16 and allowed them to regrow for another 7 to 12 days (Figure 1B). Generated iPSC-like colonies showing typical embryonic stem (ES) cell–like appearance were picked up on approximately days 21 to 28. These cells showed robust stability in phenotype, had high alkaline phosphatase (ALP) activity (Figure 1C), and expressed SSEA-1 at levels comparable with those in ES cells (supplemental Figure 1B). In the absence of leukemia inhibitory factor, they readily formed embryoid bodies (data not shown). By using a single-base polymorphism in *CD45*,[17] we could demonstrate that, of the iPSC clones thus established, 3 were derived from $Ly5.1^+$ cells and 1 from a $Ly5.2^+$ cell (Figure 1D). These results formally demonstrate that direct reprogramming of marrow hematopoietic cells is feasible given that transdifferentiation of HSCs to nonhematopoietic lineage cells is, if it ever occurs, an extremely rare event.[20] We named these iPSCs sHSC-iPS cells (sHSC-iPSCs) specifically when established from BM HSPCs reconstituted from a single HSC.

Each sHSC-iPSC clone was demonstrated to retain proviral sequences of the 4 iPSC factors (supplemental Figure 2A), without detectable transgene expression, probably resulting from gene silencing (supplemental Figure 2B). In contrast, all sHSC-iPSCs were found to express each iPSC factor gene endogenously (supplemental Figure 2B). All sHSC-iPSCs were shown to express the ES cell marker genes *Nanog*, *ERas*, *Rex1*, and *Gdf3* (supplemental Figure 3A). Nanog expression was also confirmed by immunostaining (supplemental Figure 3B). Despite the low expression levels of *Ecat1* and *Zfp296*, another set of ES cell marker genes, these sHSC-iPSCs were shown to

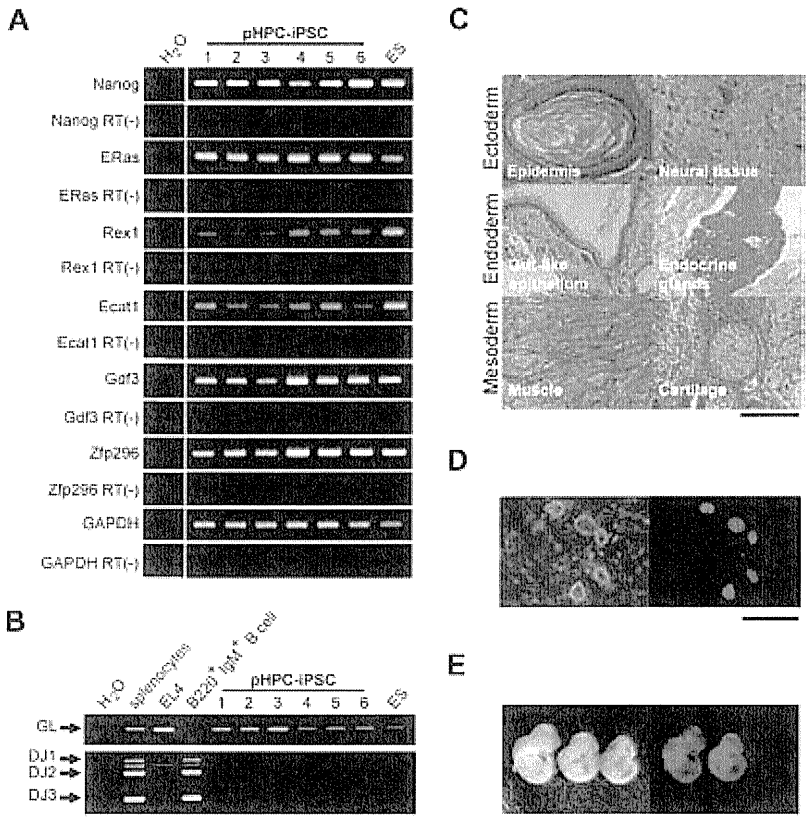

Figure 2. Characterization of primary BM hematopoietic cell–derived iPSCs generated using the 4 iPSC factors. (A) Reverse-transcription PCR analysis showing ES marker gene expression in primary BM HSPC-derived iPSC clones (pHPC-iPSCs). H_2O indicates no-template control; ES, ES cells as a positive control; RT (−), no-reverse-transcriptase control. A vertical line has been inserted to indicate a repositioned gel lane. (B) PCR analysis for Ig gene rearrangement of D-J segments (DJ1-DJ3) in pHPC-iPSC clones. GL indicates amplification of the fragment representing unrearranged, germline configuration of the Ig heavy chain gene; EL4, a T lymphoma cell line as an unrearranged control. (C) Histologic sections of teratomas derived from a pHPC-iPSC clone. (D) Images of pHPC-iPSC colonies derived from an EGFP-transgenic mouse. Bars represent 100 μm (C-D). (E) E10.5 chimeric embryos generated with one representative EGFP$^+$ iPSC clone.

be competent in both teratoma formation (supplemental Figure 4) and contribution to chimeric mice (Figure 1E).

We next sought to confirm the reproducibility of direct reprogramming of primary BM HSPCs. Lin$^-$Kit$^+$ BM cells obtained from adult B6 mice were subjected to retrovirus-mediated reprogramming procedures (Figure 1B). From approximately 5×10^5 HSPCs, we consistently obtained approximately 10 to 30 discrete colonies with typical ES cell–like appearances that stained for ALP (data not shown). Interestingly, iPSC clones established from primary BM HSPCs (pHPC-iPSCs) were shown to express ES cell marker genes more robustly than did sHSC-iPSCs (Figures 2A, S3A). Expression levels in endogenous iPSC factor genes were also more intense in pHPC-iPSCs (supplemental Figure 5B) than in sHSC-iPSCs (supplemental Figure 2B). This may support the idea that huge replicative stress imposed on a single HSC by hematopoietic reconstitution might restrict effective reprogramming of target cells, which are thought to be in senescent states. Confirmation of germline configuration in the immunoglobulin gene revealed the non–B-cell origin of pHPC-iPSCs (Figure 2B). pHPC-iPSCs had the potential for multilineage differentiation, as evidenced by the formation of teratomas, which contained various tissues representing all 3 germ layers (Figure 2C). We were also successful in generating pHPC-iPSCs that constitutively expressed green fluorescence protein from enhanced green fluorescent protein (EGFP)–transgenic mice[21] (Figure 2D). These iPSCs showed a high contribution to embryonic development when microinjected into blastocysts (Figure 2E).

Here we report generation of iPSCs from hematopoietic cells with unrearranged immunoreceptor genes by direct viral transfer of iPSC factors. The principle shown here ensures the feasibility of direct reprogramming of human hematopoietic cells, in conjunction with the recent report of iPSC generation from human blood.[8] The defined cellular origin of our iPSCs enables formal comparative studies using iPSC clones from various sources: One intriguing question is whether or not our iPSC clones differ from those generated from other tissues in respect to reprogramming efficiency, genomic stability, ability of tissue differentiation, and susceptibility to tumorigenesis. Another question is what types of cells in murine HSPCs are actually reprogrammed into iPSCs. At present, we have not yet succeeded in iPSC generation from highly purified HSCs. Considering the germline configuration of the immunoglobulin gene in our iPSC clones (Figure 2B) and the fact that the transduced cells rapidly acquired granulocytic/myeloid-lineage marker expression in our culture conditions (data not shown), myeloid progenitors are currently the plausible target cells of iPSC induction in our system. Studies to address all these issues are ongoing.

Acknowledgments

The authors thank S. Yamanaka and K. Takahashi for plasmids, R. C. Mulligan for 293GP and 293GPG cells, and H. Kawamoto and T. Ikawa for help with Ig gene analysis.

This work was supported in part by a grant from the Project for Realization of Regenerative Medicine from the Ministry of Education, Culture, Sports, Science and Technology Japan (H.N.) and by the Global Center of Excellence program from the Ministry of Education, Culture, Sports, Science and Technology Japan.

Authorship

Contribution: M. Okabe generated and characterized iPS cells; M. Otsu generated iPS cells and wrote the manuscript; D.H.A. prepared virus-producing cells; T.K. and Y.W. performed blastocyst injection; Y.M. prepared a single HSC-transplanted chimeric mouse; M. Onodera established transduction procedures

using 293GPG cells; K.E. and H.E. supported experiments with their professional knowledge and experience; and M. Otsu and H.N. supervised the study.

Conflict-of-interest disclosure: The authors declare no competing financial interests.

Correspondence: Hiromitsu Nakauchi, Division of Stem Cell Therapy, Center for Stem Cell and Regenerative Medicine, Institute of Medical Science, University of Tokyo, 4-6-1 Shirokanedai Minato-ku, 108-8639 Tokyo, Japan; e-mail: nakauchi@ims.u-tokyo.ac.jp.

References

1. Takahashi K, Yamanaka S. Induction of pluripotent stem cells from mouse embryonic and adult fibroblast cultures by defined factors. *Cell.* 2006; 126:663-676.
2. Wernig M, Meissner A, Foreman R, et al. In vitro reprogramming of fibroblasts into a pluripotent ES-cell-like state. *Nature.* 2007;448:318-324.
3. Takahashi K, Okita K, Nakagawa M, Yamanaka S. Induction of pluripotent stem cells from fibroblast cultures. *Nat Protoc.* 2007;2:3081-3089.
4. Yu J, Vodyanik MA, Smuga-Otto K, et al. Induced pluripotent stem cell lines derived from human somatic cells. *Science.* 2007;318:1917-1920.
5. Park IH, Arora N, Huo H, et al. Disease-specific induced pluripotent stem cells. *Cell.* 2008;134: 877-886.
6. Aoi T, Yae K, Nakagawa M, et al. Generation of pluripotent stem cells from adult mouse liver and stomach cells. *Science.* 2008;321:699-702.
7. Aasen T, Raya A, Barrero MJ, et al. Efficient and rapid generation of induced pluripotent stem cells from human keratinocytes. *Nat Biotechnol.* 2008; 26:1276-1284.
8. Loh YH, Agarwal S, Park IH, et al. Generation of induced pluripotent stem cells from human blood. *Blood.* 2009;113:5476-5479.
9. Hanna J, Markoulaki S, Schorderet P, et al. Direct reprogramming of terminally differentiated mature B lymphocytes to pluripotency. *Cell.* 2008;133: 250-264.
10. Onishi M, Kinoshita S, Morikawa Y, et al. Applications of retrovirus-mediated expression cloning. *Exp Hematol.* 1996;24:324-329.
11. Hamanaka S, Nabekura T, Otsu M, et al. Stable transgene expression in mice generated from retrovirally transduced embryonic stem cells. *Mol Ther.* 2007;15:560-565.
12. Nabekura T, Otsu M, Nagasawa T, Nakauchi H, Onodera M. Potent vaccine therapy with dendritic cells genetically modified by the gene-silencing-resistant retroviral vector GCDNsap. *Mol Ther.* 2006;13:301-309.
13. Sanuki S, Hamanaka S, Kaneko S, et al. A new red fluorescent protein that allows efficient marking of murine hematopoietic stem cells. *J Gene Med.* 2008;10:965-971.
14. Ory DS, Neugeboren BA, Mulligan RC. A stable human-derived packaging cell line for production of high titer retrovirus/vesicular stomatitis virus G pseudotypes. *Proc Natl Acad Sci U S A.* 1996;93: 11400-11406.
15. Kawamoto H, Ikawa T, Ohmura K, Fujimoto S, Katsura Y. T cell progenitors emerge earlier than B cell progenitors in the murine fetal liver. *Immunity.* 2000;12:441-450.
16. Schlissel MS, Corcoran LM, Baltimore D. Virus-transformed pre-B cells show ordered activation but not inactivation of immunoglobulin gene rearrangement and transcription. *J Exp Med.* 1991; 173:711-720.
17. Ramos CA, Zheng Y, Colombowala I, Goodell MA. Tracing the origin of non-hematopoietic cells using CD45 PCR restriction fragment length polymorphisms. *Biotechniques.* 2003;34:160-162.
18. Stadtfeld M, Brennand K, Hochedlinger K. Reprogramming of pancreatic beta cells into induced pluripotent stem cells. *Curr Biol.* 2008;18:890-894.
19. Osawa M, Hanada K, Hamada H, Nakauchi H. Long-term lymphohematopoietic reconstitution by a single CD34-low/negative hematopoietic stem cell. *Science.* 1996;273:242-245.
20. Wagers AJ, Sherwood RI, Christensen JL, Weissman IL. Little evidence for developmental plasticity of adult hematopoietic stem cells. *Science.* 2002;297:2256-2259.
21. Okabe M, Ikawa M, Kominami K, Nakanishi T, Nishimune Y. "Green mice" as a source of ubiquitous green cells. *FEBS Lett.* 1997;407:313-319.

Stepwise Development of Hematopoietic Stem Cells from Embryonic Stem Cells

Kenji Matsumoto[1], Takayuki Isagawa[2], Toshinobu Nishimura[1], Takunori Ogaeri[1], Koji Eto[1], Satsuki Miyazaki[3], Jun-ichi Miyazaki[3], Hiroyuki Aburatani[2], Hiromitsu Nakauchi[1]*, Hideo Ema[1]*

1 Division of Stem Cell Therapy, Center for Stem Cell and Regenerative Medicine, Institute of Medical Science, University of Tokyo, Tokyo, Japan, **2** Genome Science Division, Research Center for Advanced Science and Technology, University of Tokyo, Tokyo, Japan, **3** Division of Stem Cell Regulation Research, Osaka University Graduate School of Medicine, Osaka, Japan

Abstract

The cellular ontogeny of hematopoietic stem cells (HSCs) remains poorly understood because their isolation from and their identification in early developing small embryos are difficult. We attempted to dissect early developmental stages of HSCs using an *in vitro* mouse embryonic stem cell (ESC) differentiation system combined with inducible HOXB4 expression. Here we report the identification of pre-HSCs and an embryonic type of HSCs (embryonic HSCs) as intermediate cells between ESCs and HSCs. Both pre-HSCs and embryonic HSCs were isolated by their c-Kit$^+$CD41$^+$CD45$^-$ phenotype. Pre-HSCs did not engraft in irradiated adult mice. After co-culture with OP9 stromal cells and conditional expression of HOXB4, pre-HSCs gave rise to embryonic HSCs capable of engraftment and long-term reconstitution in irradiated adult mice. Blast colony assays revealed that most hemangioblast activity was detected apart from the pre-HSC population, implying the early divergence of pre-HSCs from hemangioblasts. Gene expression profiling suggests that a particular set of transcripts closely associated with adult HSCs is involved in the transition of pre-HSC to embryonic HSCs. We propose an HSC developmental model in which pre-HSCs and embryonic HSCs sequentially give rise to adult types of HSCs in a stepwise manner.

Citation: Matsumoto K, Isagawa T, Nishimura T, Ogaeri T, Eto K, et al. (2009) Stepwise Development of Hematopoietic Stem Cells from Embryonic Stem Cells. PLoS ONE 4(3): e4820. doi:10.1371/journal.pone.0004820

Editor: Catherine M. Verfaillie, KU Leuven, Belgium

Received November 5, 2008; **Accepted** January 31, 2009; **Published** March 16, 2009

Funding: This work was supported by grants from the Ministry of Education, Culture, Sport, Science, and Technology, Japan. These grants have no financial interests, and played no role in study and preparation of the manuscript.

Competing Interests: The authors have declared that no competing interests exist.

* E-mail: nakauchi@ims.u-tokyo.ac.jp (HN); hema@ims.u-tokyo.ac.jp (HE)

Introduction

Mammalian hematopoiesis develops in three distinct waves consisting of primitive hematopoiesis, definitive but transient hematopoiesis, and definitive and persistent hematopoiesis which is established by hematopoietic stem cells (HSCs) [1,2]. Both the first and second hematopoietic waves originate from the yolk sac where hemangioblasts, common precursors of the hematopoietic and endothelial lineages likely play a crucial role [3]. However, whether HSCs arise in either the yolk sac or the paraaortic splanchnopleure/aorta-gonad-mesonephros (P-Sp/AGM) region remains controversial [4,5,6]. The relationship between HSCs and hemangioblasts is also obscure [2,7]. In order to understand how HSCs develop in early embryos, it is important to determine the cellular origin of HSCs rather than the organ origin of HSCs.

Hematopoiesis and vasculogenesis in the early mouse embryo have been recapitulated well by *in vitro* ES differentiation systems [8,9,10]. However, generation of HSCs in substantial numbers from ESCs *in vitro* has been difficult. Kyba *et al.* were the first to report that HSCs can be efficiently generated from ESCs in the OP9 co-culture system by combining this with an inducible HOXB4 expression system (OP9 and iHOXB4 system) [11].

In concept, mesodermal cells first commit to the hematopoietic lineage before giving rise to HSCs. We provisionally called such cells pre-HSCs, and attempted to identify them in embryoid bodies (EB) using the OP9 and iHOXB4 system. We detected the potential to give rise to HSCs among c-Kit$^+$CD41$^+$CD45$^-$ cells derived from ESCs on day 6 of culture (EB6). The presence of hematopoietic progenitor activity in this population has been described [12,13,14]. The present report, however, is the first to document the presence of pre-stem cell activity but little hemangioblast activity in the c-Kit$^+$CD41$^+$CD45$^-$ cell population.

Pre-HSCs gave to an embryonic type of HSCs (embryonic HSCs) capable of reconstituting adult hematopoietic system but at a low degree. OP9 cells supported the transition of pre-HSCs to embryonic HSCs. Some genes were up- and down-regulated during the transition via enforced expression of HOXB4. Interestingly, about two-thirds of the markedly up-regulated genes were also found in our adult HSCs gene expression data. These results suggest that adult HSC-related molecules establish the very early stages of HSC development. Based on these results, we propose an HSC development model in which pre-HSCs through the stage of embryonic HSCs give rise to adult types of HSCs.

Results

Experimental design

Our basic experimental strategy consisted of EB formation, co-culture with OP9 cells, and functional assays (Fig. 1). iHOXB4 ESCs were allowed to differentiate spontaneously into EBs for 6 days without HOXB4 expression. We decided to fractionate EB6 cells mainly because by day 6 of culture the number of multipotent

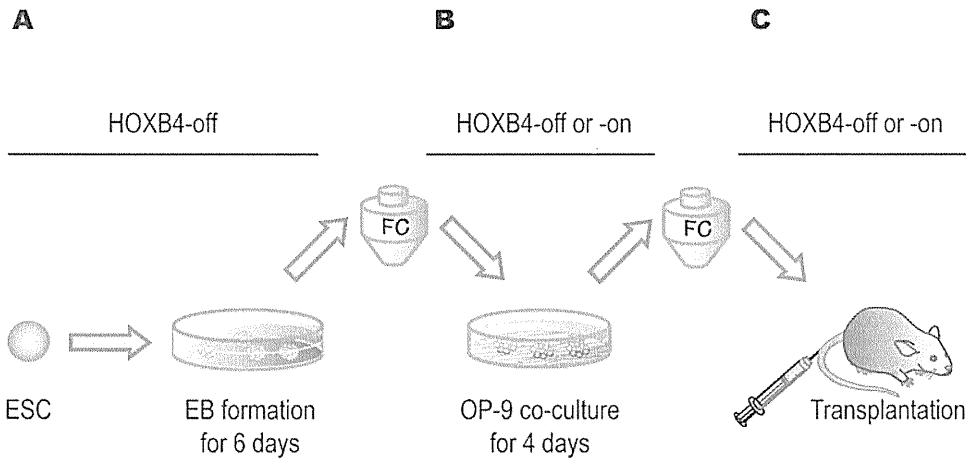

Figure 1. Study design. (A) iHOXB4 ESCs were differentiated into EBs for 6 days in the presence of Dox. (B) Dissociated EB cells were analyzed and sorted by flow cytometry (FC). EB cells or their subpopulations were co-cultured with OP9 cells for 4 days in the presence or absence of Dox. (C) Co-cultured cells were analyzed and GFP$^+$ cells were sorted by FC when HOXB4 expression was turned on. Regardless of HOXB4 status in co-cultures, FC sorting was performed on co-cultured cells based on forward and side scatters and on surface markers. Sorted cells were subjected to long-term reconstitution assays. The sorting process turned out to be useful for cell counts, removal of dead cells, and elimination of the remaining Dox.
doi:10.1371/journal.pone.0004820.g001

progenitors reaches a plateau and several surface markers become detectable (Fig. S1). CD41 is known as a marker for the initiation of definitive hematopoiesis [15,16,17,18,19]. As shown in Fig. S1, CD41 appeared in a significant proportion of EB cells on day 6 of culture. Induced HOXB4 expression during EB formation did not affect the generation of colony forming cells and repopulating cells in the OP9 and iHOXB4 system or the appearance of surface markers in EB cells. EB6 cells were analyzed and sorted by flow cytometry. Sorted EB6 cells were co-cultured with OP9 cells for various days under HOXB4-on or -off conditions. The minimal requirement of the co-culture period appeared to be only 4 days (data not shown), which is much shorter than previously thought [11]. After a second analysis and fractionation by flow cytometry, cells were subjected to *in vivo* repopulating assays under HOXB4-on or -off conditions.

The potential to give rise to HSCs in EB6 subpopulations

EB6 cells were stained with anti-CD41 antibody in combination with anti-CD45, -c-Kit, and -CD34 antibodies and others, and analyzed by flow cytometry (Fig. 2A). CD41$^+$ and CD41$^-$ cells, c-Kit$^+$CD41$^+$ and c-Kit$^-$CD41$^+$ cells, or CD34$^+$CD41$^+$ and CD34$^-$CD41$^+$ cells were sorted by flow cytometry. Sorted cells were co-cultured with OP9 cells for 4 days, and then transplanted into lethally irradiated mice along with rescue cells (Table S1) while HOXB4 expression was maintained from *in vitro* co-culture through *in vivo* repopulation.

Analysis of peripheral blood cells of the recipient mice 16 weeks after transplantation showed that c-Kit$^+$CD41$^+$ cells were enriched in cells with long-term repopulating activity (Fig. 2B). Long-term repopulating activity was similarly detected in both CD34$^-$ and CD34$^+$ cells. Lineage analysis of reconstituted mice showed that myeloid lineage reconstitution predominated. A very low level of B- and T-lymphoid lineage reconstitution was observed only in limited cases. As previously suggested, this might be due to an adverse effect of HOXB4 overexpression [11]. For long-term repopulation, HOXB4 needed to be expressed during the OP9 co-culture period and throughout the repopulation period (data not shown). All these data clearly show that c-Kit$^+$CD41$^+$ cells are the cells that require HOXB4 expression to manifest long-term repopulating activity. In addition, it should be emphasized that CD45 is not expressed in these cells (Fig. 2A).

Hemangioblasts in EB6 subpopulations

To examine whether c-Kit$^+$CD41$^+$ cells have hemangioblastic activity, we performed blast colony-forming cell (BL-CFC) assays [3] on EB6 cells under HOXB4-off or -on conditions. Unexpectedly, c-Kit$^+$CD41$^+$ cells exhibited scant BL-CFC activity, and c-Kit$^+$CD41$^-$ cells instead were significantly enriched in BL-CFC, regardless of HOXB4 expression status (Fig. 3A). The potentials to give rise to blood cells and vascular endothelial cells in BL-CFC were examined on a clonal basis as previously described [20]. Most of these blast colonies individually exhibited hematopoietic and/or endothelial differentiation potential (Fig. S2). Of note is that neither BL-CFCs nor cells composing blast colonies significantly respond to HOXB4 expression (Fig. 3A and Fig. S2). Consistent with BL-CFC data, most vasculogenic activity was detected in CD41$^-$ cells (Fig. 3B). In contrast, most primitive erythropoietic activity was detected in CD41$^+$ cells (Fig. 3C), as in the yolk sac (YS) [15], supporting the view that primitive hematopoietic progenitors arise soon after the development of mesoderm [21]. Primitive erythroid colony formation was significantly inhibited by HOXB4 expression (Fig 3C).

Genes expressed in EB6 subpopulations

RT-PCR was performed on cDNAs prepared from fractionated EB6 cells. Consistent with recently published data[14], all genes examined, including *Runx1*, *Scl*, *Gata1*, and *Gata2*, were expressed in c-Kit$^+$CD41$^+$ cells (Fig. S3), suggesting that this population at this developmental stage is already in the process of establishing definitive hematopoiesis. Expression of *Gata1*, *β-H1 globin* (*Hbb-bh1*), and *β-major globin* (*Hbb-b1*), detected in c-Kit$^-$CD41$^+$ and c-Kit$^+$CD41$^+$ cells, supports observations that these two populations contain primitive erythrocyte precursors (EryPs). *Flk1* expression with faint *Brachyury* expression in both c-Kit$^+$CD41$^-$ cells and c-Kit$^+$CD41$^+$ cells implies that these populations are the immediate progeny of mesodermal precursors. Although low levels of endogenous mouse *HoxB4* expression were detected in c-Kit$^+$CD41$^+$ cells, higher expression levels might be required for generation of HSCs.

Cell surface markers on long-term repopulating cells derived from EB cells

In order to define HSC phenotypes just before transplantation, CD41$^+$ EB6 cells were co-cultured with OP9 cells and were induced

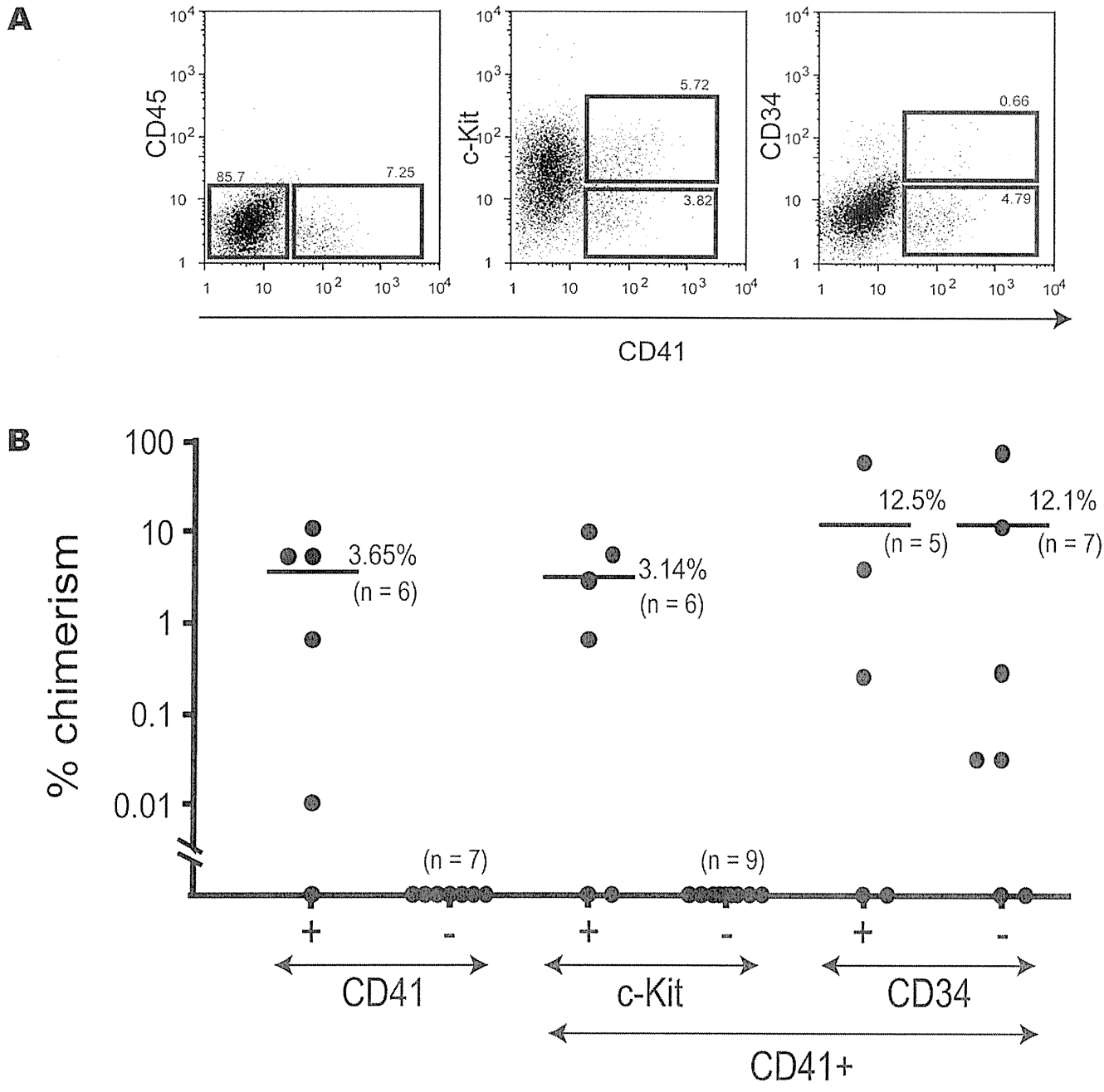

Figure 2. EB6 subpopulations with the potential of giving rise to HSCs. (A) Data from flow cytometry analysis show the expression of CD41, CD45, c-Kit, and CD34 in EB6 cells. The sorting gates for $CD41^-$ or $CD41^+$ cells, $c\text{-}Kit^+CD41^+$ or $c\text{-}Kit^-CD41^+$ cells, and $CD34^+$ $CD41^+$ or $CD34^-CD41^+$ cells are indicated as squares. **(B)** EB6 cells were fractionated based on expression of CD41, c-Kit, and CD34, co-cultured with OP9 cells for 4 days, sorted for GFP+ cells, and transplanted into lethally irradiated mice. HOXB4 expression was maintained from *in vitro* co-culture through *in vivo* repopulation. Recipient mice were analyzed 16 weeks after transplantation. Over 95% of reconstituted blood cells were of myeloid lineage in all cases (data not shown). Two independent experiments gave similar results. Data from one experiment are shown. See Table S1 for the number of transplanted cells from each subpopulation.
doi:10.1371/journal.pone.0004820.g002

to express HOXB4. HOXB4-expressing cells, detected as GFP^+ cells, were analyzed for expression of cell surface markers. GFP^+ cells were fractionated based on expression of CD41, c-Kit, CD34, or CD45 by flow cytometry (Fig. 4A) and were transplanted into lethally irradiated mice with rescue cells (Table S2). Analysis of recipient mice 16 weeks after transplantation showed that $CD41^+$ cells, $c\text{-}Kit^+$ cells, $CD34^+$ cells, and $CD45^-$ cells were enriched in long-term repopulating activity (Fig. 4B). Myeloid lineage was predominantly reconstituted in all cases. Numbers of $CD41^+$, $c\text{-}Kit^+$, and $CD34^+$ cells apparently decreased in the absence of HOXB4 expression (data not shown). These data indicate that HOXB4 expression selectively maintains the $c\text{-}Kit^+CD41^+$ $CD45^-$ phenotype and up-regulates CD34 expression during the co-culture period. It is known that fetal liver HSCs express CD34 antigen while adult bone marrow HSCs barely express CD34 antigen [22,23]. These data suggest that ESC-derived HSCs remain phenotypically immature.

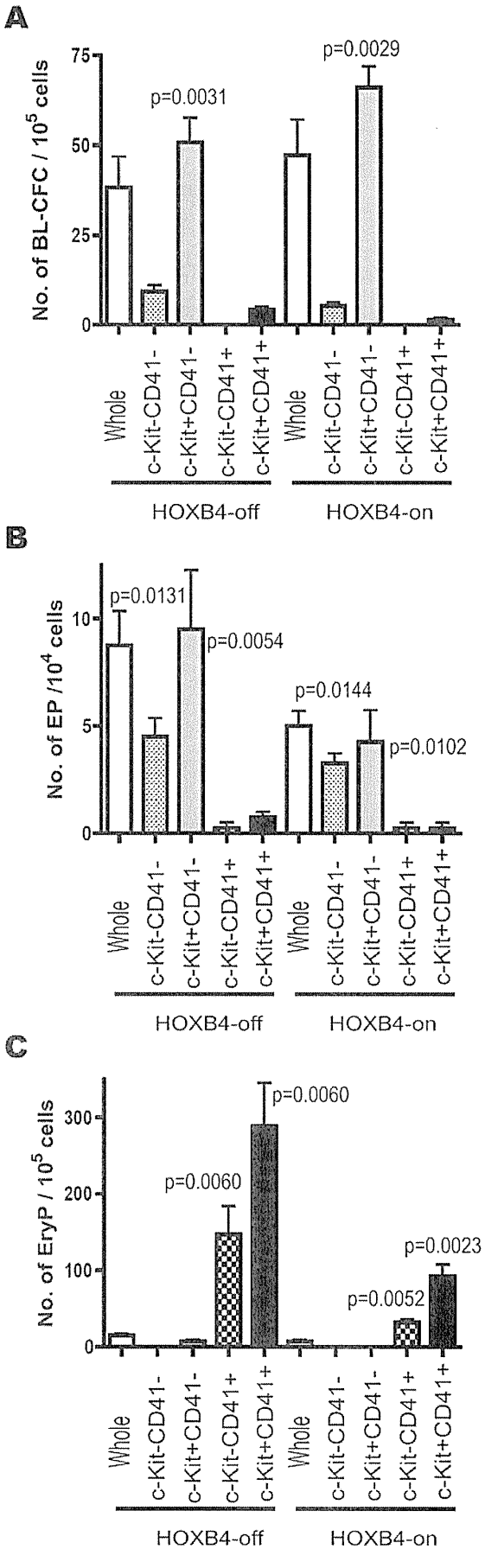

Figure 3. Hemangioblastic, endothelial, and primitive erythrocytic potentials among EB6 subpopulations. Colony forming abilities in unfractionated, c-Kit$^-$CD41$^-$, c-Kit$^+$CD41$^-$, c-Kit$^-$CD41$^+$, or c-Kit$^+$CD41$^+$ EB6 cells were examined in quadruplicate. **(A)** Blast colony-forming assays were performed. **(B)** Vascular endothelial progenitors (EP) were detected by the OP9 co-culture system with cytokines as previously described [20]. **(C)** Erythroid colonies were detected by methylcellulose colony assays. Detected erythroid colonies contained primitive erythrocytes as identified by *β-H1 globin* expression (data not shown). Kruskal-Wallis testing was performed for statistical analysis.
doi:10.1371/journal.pone.0004820.g003

In vivo function of HSCs derived *in vitro* from ESCs

We observed that c-Kit$^+$CD41$^+$ cells had accumulated in the bone marrow of recipient mice when analyzed 18 weeks after transplantation (Fig. S4). We attempted to shut HOXB4 expression off in recipient mice from 8 to 14 weeks after transplantation by letting them drink water containing 100 μg/ml of Dox. Analysis of peripheral blood cells from these mice showed that GFP$^+$ cells became undetectable and that B- and T-lymphoid lineage reconstitution was significantly improved. Myeloid lineage reconstitution, contrariwise, was reduced, with decreases in total chimerism (data not shown). After GFP$^+$ bone marrow cells were isolated from other mice reconstituted with ESC-derived cells, 1.2×10^5 GFP$^+$ cells together with 2×10^5 rescue cells was transplanted into each of 6 lethally irradiated mice, of which 3 were given Dox and 3 were not. Of the 3 recipients given Dox, 2 mice showed 0.8% and 15% chimerism, with respectively 46 : 54% and 50 : 50% myeloid : lymphoid lineages. Of the 3 recipients not given Dox, 4 mice showed 45% and 83% chimerism with almost exclusively myeloid lineage. These results support the hypothesis that HOXB4 expression negatively affects lymphoid differentiation and positively affects repopulating activity in ES-derived HSCs [11], effects not seen in adult HSCs [24].

HOXB4 target genes in HSC development

Our last experiments compared gene expression profiling among c-Kit$^+$CD41$^+$ EB6 cells (cells with the potential to give rise to HSCs), c-Kit$^+$CD41$^+$ cells after co-culture with HOXB4 expression (repopulating cells), and c-Kit$^+$CD41$^+$ cells after co-culture without HOXB4 expression (non-repopulating cells). We attempted to identify candidate genes whose expression is up- or down-regulated by HOXB4, among which might exist important genes that control the early development of HSCs. To verify the Tet-off strategy, HOXB4 expression was examined in these 3 populations and in ESCs maintained in the presence of Dox (ESCs without HOXB4 expression). As expected, *HOXB4* expression was only detected in c-Kit$^+$CD41$^+$ EB6 cells after co-culture without Dox (Fig. S5).

Microarray analysis was performed on cDNAs prepared from c-Kit$^+$CD41$^+$ EB6 cells without HOXB4 expression and c-Kit$^+$CD41$^+$ cells after co-culture with or without HOXB4 expression. In order to focus on genes up- and down-regulated by HOXB4 expression, we employed stringent criteria (Legends, Tables S3 and S4). Genes with 5-fold or more difference in gene chip scores between c-Kit$^+$CD41$^+$ cells after co-culture with HOXB4 expression and c-Kit$^+$CD41$^+$ cells without HOXB4 expression were selected.

After selection, 294 and 115 probes, respectively, remained for HOXB4 up- and down-regulated genes. We next examined whether these selected genes are expressed in HSCs via gene expression profiling of adult HSCs. HSC-expressing genes shared 200 of 294 probes for HOXB4 up-regulated genes. Of great interest is that *CD34*, *CD150* (*Slamf1*), *c-Mpl*, *integrin α4* and *α6* (*Itga4* and *6*), and *transforming growth factor β type II receptor* (*Tgfbr2*) were among them. On the other hand, 58 of 115 probes for down-regulated genes by HOXB4 were not detected on adult HSC

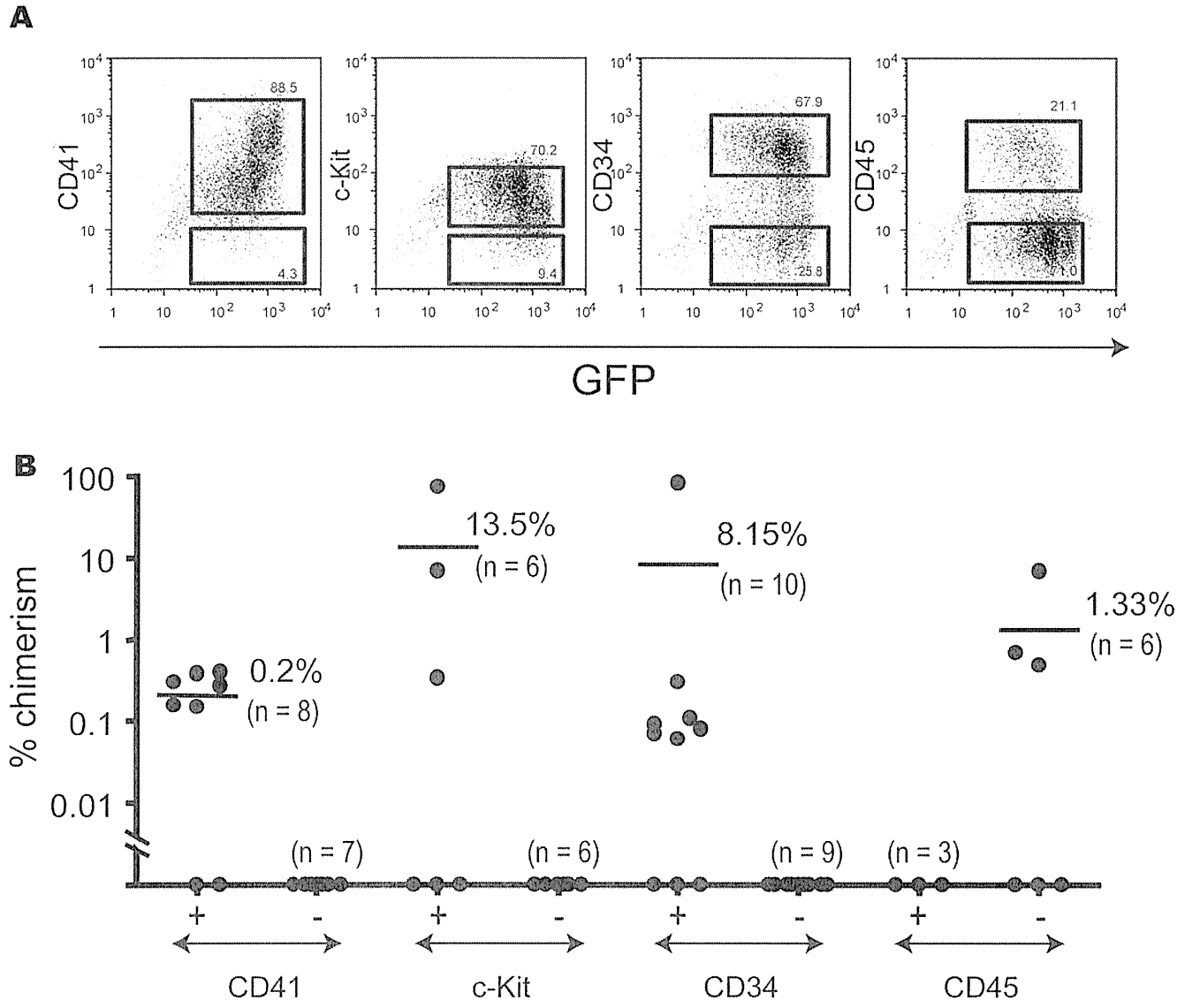

Figure 4. Surface markers of embryonic HSCs generated from EB6 cells *in vitro*. **(A)** $CD41^+$ EB6 cells were co-cultured with OP9 cells in the absence of Dox for 4 days. Cells collected from the co-cultures were analyzed by flow cytometry. HOXB4-expressing cells were detected by GFP expression. Data show the expression of CD41, c-Kit, CD34, and CD45 in GFP^+ cells. The sorting gates for $CD41^-$ or $CD41^+$ cells, c-Kit^- or c-Kit^+ cells, $CD34^-$ or $CD34^+$ cells, and $CD45^-$ or $CD45^+$ cells are shown as squares. **(B)** Co-cultured cells were fractionated based on expression of CD41, c-Kit, CD34, and CD45, and were transplanted into lethally irradiated mice. Recipient mice were analyzed 16 weeks after transplantation. Over 95% of reconstituted blood cells were of myeloid lineage in all cases (data not shown). Two independent experiments gave similar results. Data from one experiment are shown. See Table S2 for the number of transplanted cells for each subpopulation.
doi:10.1371/journal.pone.0004820.g004

profiling. All up-regulated adult HSC-related genes and all down-regulated adult HSC-unrelated genes are listed in Tables S3 and S4 and are also schematically presented as a heat map in Fig. 5A. The overall similarity in the heat map between the EB6 and the HOXB4-off samples suggests that these data represent the effect of enforced expression of HOXB4. RT-PCR analysis showed that the expression levels of *CD150* and *c-Mpl* were significantly higher in HOXB4-on c-Kit^+CD41^+ cells than in HOXB4-off c-Kit^+CD41^+ cells, and that the expression levels of *βh1-globin* (*Hbb-bh1*) and *Lin28* were significantly lower in HOXB4-on c-Kit^+CD41^+ cells than in HOXB4-off c-Kit^+CD41^+ cells (Fig. 5B). A marked increase in $CD34^+$ repopulating cells (Fig. 4) and a marked decrease in primitive erythroid progenitors (Fig. 3) with HOXB4 expression were consistent with the gene expression profiling data.

A number of genes are implicated as playing important roles in the generation of HSCs. According to our microarray data, significant levels of Scl, Runx1, Gata2, or Lmo2, were expressed in c-Kit^+CD41^+ cells, but induced HOXB4 expression did not change their expression levels. Expression levels of Cdx1 and Cdx4 remained low in c-Kit^+CD41^+ cells regardless of HOXB4 expression.

Discussion

This study demonstrates that pre-HSCs, perhaps conceptually relevant to hemogenic endothelium [25], can be prospectively isolated from developing mouse EBs. Pre-HSCs were unable to engraft and to reconstitute the hematopoietic system in lethally

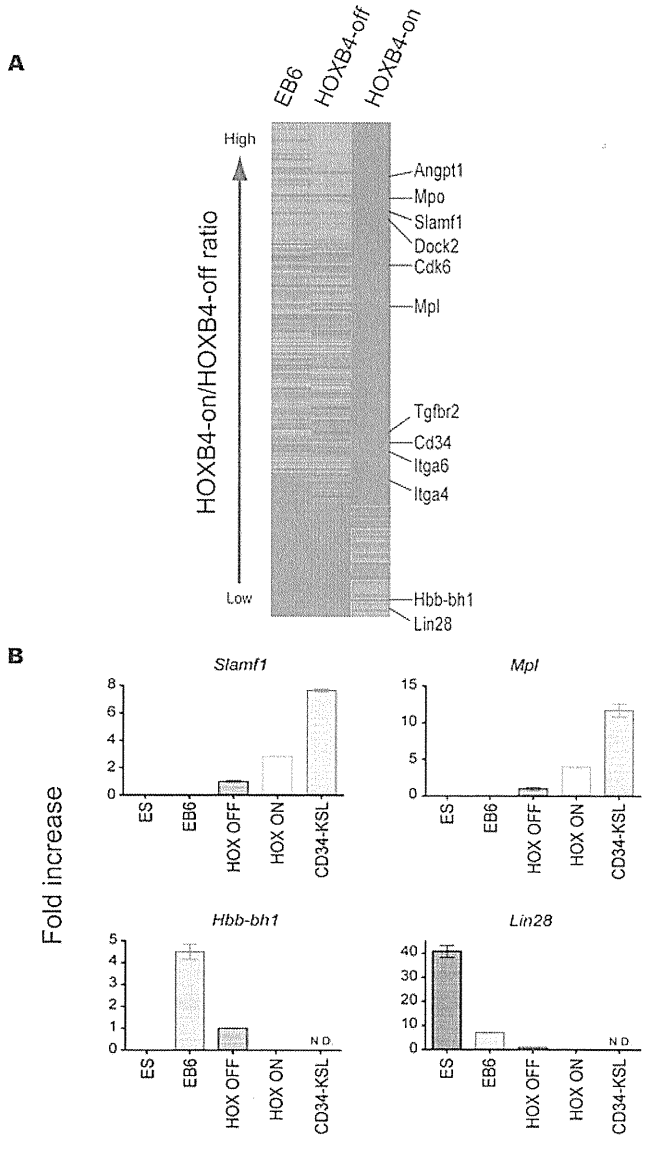

Figure 5. Heat map of differentially expressed genes. (A) Microarray analysis was performed on cDNAs from c-Kit$^+$CD41$^+$ EB6 cells without HOXB4 expression, c-Kit$^+$CD41$^+$ cells after co-culture without HOXB4 expression, and c-Kit$^+$CD41$^+$ cells after co-culture with HOXB4 expression. The finally selected 223 genes are shown in this graph (for selection criteria, see Legend, Table S3). Red indicates genes up-regulated 5-fold or more. Blue indicates genes down-regulated 5-fold or more. **(B)** Real-time PCR was performed on normalized cDNA from the cells described above, from ESCs maintained without HOXB4 expression, and from CD34$^-$KSL cells from adult bone marrow. The mean plus or minus 1SD (n = 3) is shown for 4 representative genes.
doi:10.1371/journal.pone.0004820.g005

irradiated adult mice. To engraft in adult mice, pre-HSCs should acquire both engraftment and repopulating capacities. This developmental process was driven or enhanced by enforced expression of HOXB4. Contrary to previous studies [11], HOXB4 had to be continuously expressed *in vivo* after transplantation to maintain long-term repopulation in this study. When HOXB4 expression was turned off in some reconstituted mice, myeloid reconstitution level was decreased while B- and T-lymphoid reconstitution levels were increased. As a result, the total chimerism was gradually reduced (data not shown). We used a Tet-off system while Kyba et al. used a Tet-on system. An explanation for this discrepancy may be that Tet-on systems are "leaky" by comparison with Tet-off systems, permitting weak persistent expression of HOXB4 even after turn-off in the work of Kyba *et al.* Long-term repopulating cells generated from pre-HSCs by OP9 co-culture and HOXB4 expression persistently showed low levels of long-term reconstitution. When 10^5 adult bone marrow cells, instead of Sca-1$^-$ rescue cells, were used as competitor cells, reconstitution became undetectable (data not shown). A similar property has been observed for HSCs from the YS and P-Sp/AGM region. We operationally called these HSCs with low repopulating potential embryonic HSCs.

As previously noticed [11], HOXB4 overexpression seemed to have prevented lymphoid reconstitution, with long-term reconstitution mainly myeloid in this study. Multilineage reconstitution has been a criterion for HSCs. However, myeloid reconstitution may be more reliable than lymphoid reconstitution as a marker of HSC activity because short-lived granulocytes are never detectable in the circulation for long unless they are continuously supplied by engrafted HSCs.

Pre-HSCs and embryonic HSCs are distinct populations in function and gene expression profiling, but they both exhibited the c-Kit$^+$CD41$^+$CD45$^-$ phenotype. Since c-Kit is already expressed in a significant proportion of undifferentiated ESCs and in most YS, P-Sp/AGM, fetal liver, and adult bone marrow HSCs [6,26,27,28], the maintenance of this receptor tyrosine kinase may be crucial for the development of HSCs from the internal cell mass.

CD41 marks both primitive and definitive hematopoiesis [15,16,17,18]. The developmental wave of definitive but transient hematopoiesis clearly differs from that of HSCs [1,2]. Whether CD41 also marks HSCs in their early development has been uncertain. In this study, pre-HSCs and primitive erythroid progenitors were detected among CD41$^+$ cells (Figs. 2B, 3C). In contrast, hemangioblastic and vasculogenic activities were principally detected in CD41$^-$ cells.

Hemangioblasts are thought to play a major role in initiation of primitive and definitive hematopoiesis [3]. HSCs have been generally believed to arise from hemangioblasts [7]. Unlike previous studies[3], our blast colony assays were performed on EB6 cells instead of EB3.0 or 3.5 cells. This might be the reason that pre-HSC and hemangioblast activities were detected in the separated populations. Pre-HSCs may develop closely associated with hemangioblasts because these two types of cells arise from common mesodermal precursors at a very early point. It is important to clarify at which stage these cell classes separate from one another during development. Our data suggest that pre-HSCs are separated from hemangioblasts as soon as they arise. The possibility exists that pre-HSCs initially develop through hemangioblasts, but soon thereafter these two types of cells become distinct from one another. Alternatively, HSCs develop independent of hemangioblasts. Since *in vitro* differentiation of ESCs along the blood lineage mostly mimics YS hematopoiesis [29], it is possible that pre-HSCs arise in close association with YS development. In this case, pre-HSCs presumably are unable efficiently to differentiate into embryonic HSCs in the YS microenvironment, but, after migration, are able to do so in particular developmental niches like the P-Sp/AGM region [4,5] and the fetal liver microenvironment.

Although fetal and adult HSCs express CD45, pre-HSCs and embryonic HSCs were shown not to express CD45. Most HSCs from the YS and P-Sp/AGM region at E10.5 or earlier do not express CD45 [19,30]. In this regard, CD45 is a late maturation marker of HSCs whereas CD41 is an early maturation marker of HSCs. Identification and characterization of c-Kit$^+$CD41$^+$CD45$^-$ pre-HSCs and embryonic HSCs in early developing embryos will clarify the significance of changes in HSC phenotype.

We and others have been interested in target genes of HOXB4. If other HSC inducers are indentified among such molecules, more efficient generation of HSCs should become possible. A large number of candidate target genes has been reported recently [31]. Unfortunately, these expressed genes were not always identified among populations properly enriched in HSC activity. We therefore used c-Kit$^+$CD41$^+$ cells from which HSC activity emerged after HOXB4 expression was turned on.

Among a number of candidate genes obtained in this study were many genes known to be expressed in adult HSCs (Table S3). Of special note is that *CD34*, *CD150*, and *c-Mpl* are up-regulated in the transition of pre-HSCs to embryonic HSCs. Only some pre-HSCs expressed CD34, but all embryonic HSCs derived from pre-HSCs expressed CD34 (Fig. 4). That CD34 is expressed in YS and P-Sp/AGM HSCs [6,32] supports the inference that all these cells are closely related. CD150, which is expressed from fetal HSCs to adult HSCs, is a new HSC marker [33,34]. c-Mpl, the receptor for TPO, is expressed in most fetal and adult HSCs. Although the function of CD34, CD150, or c-Mpl is not essential for the development of HSCs [12,35,36], it is suggested that these HSC markers begin to be expressed at the embryonic HSC stage. CD34, CD150, and c-Mpl could be good candidates for the earliest markers during HSC development. Since many intracellular molecules (*e.g.*, angiopoietin 1 and myeloperoxidase) were also up-regulated, they might also serve as markers for embryonic HSCs. Angiopoietin 1, secreted by HSCs in the P-Sp/AGM region, fetal liver, and adult bone marrow, has been suggested to promote angiogenesis [37]. High levels of expression of these molecules might be tightly associated with commitment to HSC lineage. The origin of HSCs – YS or P-Sp/AGM region – has been debated for a very long time. It is difficult to determine precisely which site is the first origin of HSCs because in the mouse embryo the P-Sp/AGM region does not exist at E7, when the YS begins to appear. A combination of markers listed in this study should be useful for *in vivo* detection of embryonic HSCs.

Fetal and adult HSCs are functionally distinct [38,39]. Pre-HSCs and embryonic HSCs are functionally different from fetal and adult HSCs. Our working model for HSC development is presented in Fig. 6. We propose that pre-HSCs which arise from mesoderm, possibly independent of hemangioblasts, give rise to embryonic HSCs which subsequently give rise to fetal and adult HSCs. Whether all adult HSCs are generated by fetal HSCs remains uncertain, as recently suggested [40]. These processes should take place in spatially and temporally established niches in developing embryos. Certainly much more work is required, but identification and characterization of pre-HSCs and embryonic HSCs in developing embryos are central to validation of this model.

Embryonic stem cells (ESCs) hold great promise to innovate a variety of new therapies for regenerative medicine because of their potential of differentiating into all sorts of adult cells. The key to success in stem cell therapy is to establish methods of properly differentiating ESCs into any particular type of tissue-specific stem cells. Recent establishment of induced pluripotent stem cell lines [41,42] demands more such protocols. In order to generate HSCs from ESCs efficiently *in vitro*, optimal conditions must be determined for each developmental step in our model.

Materials and Methods

Mice

129/OlaHsd (129Ola) mice were purchased from Jackson Laboratory (Bar Harbor, ME). Ly5 congenic C57BL/6 mice (B6-Ly5.1) were obtained from Sankyo Laboratory Service (Tsukuba, Japan). 129Ola and B6-Ly5.1 mice were mated to produce F1 mice (Ly5.1×Ly5.2). Mice were maintained in the Institute of Medical Science University of Tokyo Animal Research Center. All experiments using mice received approval from the Institute of Medical Science Animal Experiment Committee.

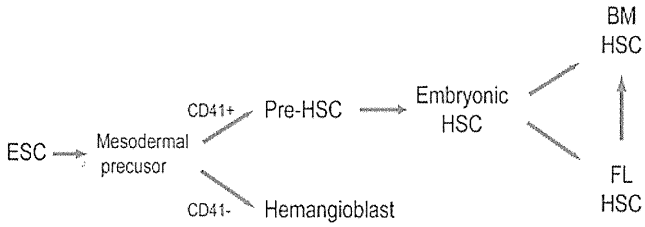

Figure 6. A stepwise developmental model for HSCs. We propose a working model for HSC development. Pre-HSCs originate from mesoderm, possibly independent of hemangioblasts; pre-HSC give rise to embryonic HSCs in particular niches in the YS or P-Sp/AGM region; embryonic HSCs give rise to fetal and adult HSCs in particular niches in the fetal liver and bone marrow.
doi:10.1371/journal.pone.0004820.g006

ESCs

The mouse ES cell line EB3, derived from E14tg2a ESCs, was maintained without mouse embryonic fibroblasts in Glasgow minimum essential medium supplemented with 10% fetal calf serum (FCS) (JRH Bioscience, Lenexa, KS), 0.1 mM 2-mercaptoethanol (2-ME), 2 mM L-glutamine (L-Gln), 0.1 mM non-essential amino acids, 1 mM sodium pyruvate (Invitrogen, Carlsbad, CA), 1,000 U/ml leukemia inhibitory factor (LIF, Chemicon, Temecula, CA), and 100 U/ml penicillin/streptomycin. For these cultures, a 100 mm-tissue culture dish was used after coating with 5 ml of 0.1% gelatin in PBS for 10 min at 37°C.

Tet-regulated HOXB4/GFP expression in ESCs

The tetracycline (Tet)-off system was chosen because gene expression is more strictly controllable in the Tet-off system than in the Tet-on system [43]. ESCs carrying the Tet-off iHOXB4 expression cassette in the ROSA26 locus (iHOXB4 ESCs) were made as previously described (Fig. S6) [44].

In vitro ESC differentiation

iHOXB4 ESCs were maintained in the presence of 1 μg/ml doxycycline (Dox), a tetracycline derivative. To allow ESCs to differentiate into EBs, ESCs were trypsinized and collected in complete EB differentiation medium (EBD) [3]. Cells were transferred into a 100-mm Petri dish at 2×10^5 cells per 10 ml EBD. The medium was changed on day 4 of culture and every 2 days thereafter.

Co-culture with OP9 cells

OP9 cells were maintained in α-MEM containing 15% FCS. 10^5 OP9 cells were plated in each well of a 6-well tissue culture plate 2 days before starting co-culture. Developed EBs were treated with 0.25% trypsin for 4 min at 37°C and were disrupted to yield single cells. Co-cultures were employed with IMDM containing 20 ng/ml mouse stem cell factor (SCF) and 20 ng/ml human thrombopoietin (TPO), 10% FCS, 2 mM L-Gln, 0.1 mM 2-ME, and 100 U/ml penicillin/streptomycin. On specified days of co-culture, cells were recovered from the culture dishes for analysis and sorting on a flow cytometer.

Flow cytometry analysis and sorting

ESCs, EB cells, and cells after OP9 co-culture were stained with phycoerythrin-conjugated (PE-) anti-Flk-1 (eBioscience, San

Diego, CA), allophycocyanin-conjugated (APC-) anti-CD31, biotinylated anti-CD34, PE-anti-CD41, and APC-anti-c-Kit antibodies (BD Biosciences, San Jose, CA) on ice for 30 min. Streptavidin-APC-Cy7 (BD Biosciences) was used for detection of biotinylated antibody. Analysis and sorting were performed on a MoFlo (DAKO, Glostrup, Denmark).

Methylcellulose colony assays

Cells were cultured in 1% methylcellulose containing 30% FCS, 1% bovine serum albumin, 2 mM L-glutamine, and 0.05 mM 2-ME. For colony assays, 10 ng/ml mouse interleukin-3, 10 ng/ml SCF, 2 U/ml human erythropoietin, and 50 ng/ml TPO were included. Cells were incubated at 37°C in a humidified atmosphere with 5% CO_2 in air. Colonies were counted on day 10 of culture and individually picked up. Each colony was cytocentrifuged onto a glass slide for morphological examination with May-Gruenwald-Giemsa staining. Primitive erythroid colonies were counted on day 3 of culture. Blast colony assays were performed as previously described [16]. In brief, cells were cultured in IMDM containing 1% methylcellulose, 10% FCS, 4.5×10^{-4} M monothiolglycerol, 1% L-Gln, 25 μg/ml ascorbic acid, 300 μg/ml human saturated transferrin, 5 ng/ml vascular endothelial growth factor, 100 ng/ml SCF, and 5 ng/ml IL-6. Blast colonies were counted on day 4 of culture.

Long-term reconstitution assays

2- to 3-month-old B6-Ly5.1×129Ola F1 mice (Ly5.1/Ly5.2) were irradiated at a dose of 900 cGy. ES-derived cells (Ly5.2) were transplanted into these mice (Ly5.1/ly5.2) along with 3×10^5 Sca-1-depleted (Sca-1$^-$) bone marrow cells from B6-Ly5.1×129Ola F1 mice as rescue cells. To prepare Sca-1$^-$ cells, mononucleated cells were obtained by density gradient centrifugation using Ficoll-Paque PLUS (Amersham Biosciences, Uppsala, Sweden). Cells were stained with anti-Sca-1 antibody-conjugated magnetic beads (Miltenyi Biotec, Bergisch Gladbach, Germany). Sca-1$^+$ cells were magnetically depleted using an LD column (Miltenyi Biotec).

Peripheral blood cells from recipient mice were analyzed 4 and 16 weeks after transplantation. After red blood cell lysis, cells were stained with biotinylated anti-CD45.1 antibody. After washing, cells were stained with PE-anti-CD4, PE-anti-CD8, APC-anti-Gr-1, APC-anti-Mac-1, and PE-Cy7-anti-B220 antibodies and with APC-Cy7-streptavidin. At least 10^5 cells were analyzed, and data were collected on a FACS Aria (BD Biosciences). Test donor cells' contribution was detected with the GFP marker. Percentage chimerism was defined as percentage of GFP$^+$ cells in peripheral leukocytes. Test donor cells were considered to have contained long-term repopulating cells when chimerism was over 0.01%.

RT-PCR

PCR was performed on cDNAs from sorted cells as previously described [45]. Primers are listed in Table S5. The PCR program consisted of 38 cycles of 15 sec at 95°C, 15 sec at 56°C, and 20 sec at 72°C.

Real-time PCR

The PCR primers were designed using a program provided by Roche (https://www.roche-applied-science.com/sis/rtpcr/upl/index.jsp). PCR contained normalized cDNAs, Universal Probe Library Set, and FastStart Universal Probe Master (Roche, Basel, Switzerland). Quantitative PCR analyses were performed in real-time using an ABI PRISM 7900HT (Applied Biosystems, Foster City, CA). The PCR program consisted of 43 cycles of 15 sec at 95°C and 60 sec at 60°C. Each value was divided by the mean value from HOXB4-off samples to be expressed as fold increase.

Microarray analysis

Total RNA was extracted from 3 sets of cells. The first was c-Kit$^+$CD41$^+$ EB6 cells derived from iHOXB4 ESCs without HOXB4 expression. The second and third were c-Kit$^+$CD41$^+$ cells after co-culture with OP9 cells for 4 days with or without HOXB4 expression. To prepare cells in the last 2 groups, c-Kit$^+$CD41$^+$ EB6 cells were plated onto a monolayer of OP9 cells and were cultured either in the presence or absence of Dox for 4 days. c-Kit$^+$CD41$^+$ cells were again separated from the co-cultures by flow cytometry. To compare gene expression profiles with those of adult HSCs, CD34$^-$c-Kit$^+$Sca-1$^+$Lineager marker$^-$ (CD34$^-$KSL) cells were isolated from C57BL/6 mice as previously described [26]. In order to analyze cycling adult HSCs, CD34$^-$KSL cells were incubated with 50 ng/ml SCF and 50 ng/ml TPO for 24 hours [46]. Integrity of RNA was assessed qualitatively on an Agilent 2100 Bioanalyzer (Agilent Technologies, Santa Clara, CA). cDNA was synthesized with a MessageAmp aRNA Kit (Applied Biosystems). *In vitro* transcription and labeling were performed using One-Cycle Target Labeling and Control Reagents (Affymetrix, Santa Clara, CA) for ESCs and ESC-derived cells, and using Tow-Cycle Target Labeling and Control Reagents (Affymetrix) for adult HSCs. The heat-fragmented probes were hybridized to a Mouse Genome 430 2.0 GeneChip (Affymetrix). The arrays were scanned and analyzed with the Affymetrix GeneChip System. The relative abundance of each gene was estimated from the average difference of intensities.

Statistical analysis

Mann-Whitney testing was performed when two groups were compared. Kruskal-Wallis testing was performed when multiple groups were compared.

Supporting Information

Table S1
Found at: doi:10.1371/journal.pone.0004820.s001 (0.02 MB PDF)

Table S2
Found at: doi:10.1371/journal.pone.0004820.s002 (0.02 MB PDF)

Table S3
Found at: doi:10.1371/journal.pone.0004820.s003 (0.18 MB PDF)

Table S4
Found at: doi:10.1371/journal.pone.0004820.s004 (0.06 MB PDF)

Table S5
Found at: doi:10.1371/journal.pone.0004820.s005 (0.03 MB PDF)

Figure S1 Effect of HOXB4 expression in generation of CFU-nmEM and surface marker expression. (A) Data show colony formation by 1,000 cells derived from EB. 1,000 cells were obtained from EBs on days 0, 2, 4, 5, 6, and 7 of culture and co-cultured with OP9 cells for 4 days. Cells collected from the co-cultures were plated in methylcellulose. HOXB4 expression was turned off in both OP9 co-cultures and methylcellulose cultures (HOXB4-off), turned on in both (HOXB4-on), or turned on only in OP9 co-cultures (HOXB4-on to -off). The number of colonies was counted and cells composing each colony were morphologically examined. The graphs show the numbers of neutrophil/macrophage/erythroblasts/megakaryocyte (nmEM) colonies extracted from various colonies formed. Continuous expression of HOXB4 in methylcellulose culture was not necessary for nmEM colony formation. The number of colonies is the mean from 2 independent experiments. (B) Cell surface markers were examined during EB formation without HOXB4 expression. Flk-1+ cells were first detected on day 3 of culture; the proportion of Flk-1+ cells markedly increased on the following day and decreased

thereafter. CD31+ cells and CD41+ cells became detectable by day 5 and day 6, respectively, followed by the appearance of CD34+ cells. CD45+ cells became detectable after day 6, but remained low in number. c-Kit+ cells constituted about half of the cells throughout EB formation regardless of whether HOXB4 expression was induced (data not shown).
Found at: doi:10.1371/journal.pone.0004820.s006 (9.39 MB TIF)

Figure S2 Differentiation potential of individual blast colonies. Both hematopoietic and endothelial potentials were examined for individual blast colonies. Blast colonies were formed by whole EB6 cells (Fig. 3A). Colonies were individually picked up from methylcellulose and co-cultured with OP9 cells in the presence of vascular endothelial growth factor, stem cell factor, interleukin-3, TPO, and erythropoietin for 7 days. (A) The summary of hematopoietic and endothelial potentials detected in individual blast colonies. (B) Representative photomicrographs show that a colony consisted of blood cells and CD31-positive vascular endothelial cells.
Found at: doi:10.1371/journal.pone.0004820.s007 (6.61 MB TIF)

Figure S3 RT-PCR for 4 EB6 cell populations. PCR was performed on cDNAs prepared from fractionated EB6 cells.
Found at: doi:10.1371/journal.pone.0004820.s008 (3.55 MB TIF)

Figure S4 Analysis of bone marrow cells from recipient mice of HOXB4-expressing ES-derived cells. c-Kit+CD41+ EB6 cells were co-cultured with OP9 cells while HOXB4 was enforcedly expressed. After co-culture with OP9 cells, GFP+ cells and rescue cells were transplanted into lethally irradiated mice. 18 weeks after transplantation, bone marrow cells of the recipient mice were stained with antibodies and analyzed on a flow cytometer. (A–E) GFP− cells were derived from rescue cells and possibly from host cells. (F–J) GFP+ cells were derived from ESCs. GFP− cells and GFP+ cells are separately displayed for the expression of Gr-1 and Mac-1 (A, F), B220 and CD19 (B, G), CD4 and CD8 (C, H), Sca-1 and c-Kit (D, I), and CD41 and CD45 (E, J).
Found at: doi:10.1371/journal.pone.0004820.s009 (1.28 MB TIF)

Figure S5 RT-PCR analysis for induced HOXB4 expression in c-Kit+CD41+ cells. ESCs were maintained in the presence of Dox (ES HOXB4-off). After ESCs were differentiated into EB6 cells in the presence of Dox, c-Kit+CD41+ cells were isolated (c-Kit+CD41+ EB6 HOXB4-off). These cells were co-cultured with OP9 cells in the presence or absence of Dox for 4 days, followed by recovery of c-Kit+CD41+ cells from the co-cultures (c-Kit+CD41+ HOXB4-off and c-Kit+CD41+ HOXB4-on). These c-Kit+CD41+ cells and ESCs along with adult bone marrow cells (Total BM) as a negative control were examined for HOXB4 expression by RT-PCR analysis. The PCR program consisted of 15 sec at 95°C, 15 sec at 60°C, and 30 sec at 72°C. A total of 42 cycles or 30 cycles was used for amplification of HOXB4 or Gapdh.
Found at: doi:10.1371/journal.pone.0004820.s010 (9.28 MB TIF)

Figure S6 Tet-off inducible HOXB4/EGFP expression system. (A) Schematic presentation of the Tet-off HOXB4 gene expression cassette integrated into the constitutive active ROSA 26 locus on chromosome 6. HOXB4 cDNA was kindly provided by Dr. K. Humphries (Terry Fox Laboratory, Vancouver, Canada). The Tet-off regulated gene expression plasmid comprised a splice-acceptor (SA) sequence; a loxP-flanked neomycin phosphotransferase gene (neor) gene, including a polyA signal; the Tet-controlled transcriptional activator (tTA) gene, including a polyA signal; an insulator sequence; the tTA-responsive element (TRE), followed by the minimal immediate-early promoter from Cytomegalovirus (CMV); the rabbit beta-globin 2nd intron; human HOXB4 cDNA; an internal ribosome entry site (ires); EGFP cDNA; and a polyA signal. The constructed vector was amplified in E. coli Stabl2 cells (Invitrogen), purified using a GENOPURE plasmid maxi kit (Roche), linearized by SwaI digestion, and used to transfect ESCs. The Tet-regulated HOXB4/EGFP expression cassette was integrated into the constitutively active ROSA26 locus in EB3 cells by homologous recombination. In brief, EB3 ESCs were electroporated with the linearized vector and were selected with G418 (150–200 μg/ml). G418-resistant colonies were picked and ES clones carrying a targeted integration of the vector in the ROSA26 locus were identified by long distance-PCR analysis using the following primers: forward (ROSA26 locus 1st exon), 5′-CCTCGGCTAGG-TAGGGGATCGGGACTCT-3′; reverse (neor gene), 5′-CGGA-GAACCTGCGTGCAATCCATCTTGTTC-3′; forward (EGFP), 5′-GGATCACTCTCGGCATGGACGAGCTGTAC-3′; and reverse (ROSA26 locus 2nd exon), 5′-AGCCTTAAACAAG-CACTGTCCTGTCCTCAAG-3′. The PCR cycles consisted of one cycle at 94°C for 1 min, 32 cycles at 98°C for 20 s, 66°C for 30 s, 68°C for 4 min, and one cycle at 72°C for 10 min. To remove the loxP-flanked neor gene, Cre recombinase was transiently expressed in the selected clones by transfection with the pCAG-cre-IRES-puro plasmid. The resultant ES cell line was named "inducible HOXB4-EGFP ESCs" (iHOXB4 ESCs). (B) In the absence of doxycycline (Dox), tTA binds to the TRE, resulting in activation of HOXB4/EGFP transcription. In the presence of Dox, Dox binds tTA, preventing tTA binding to the TRE. We tested if this inducible expression system works in HOXB4 ES clones. Representative results from Western blot analysis for 4 clones are shown. HOXB4 was not detected when ESCs were cultured in the presence of Dox. HOXB4 was detected when ESCs were cultured in the absence of Dox. Anti-FLAG antibody was used to detect HOXB4. EGFP expression in these ES clones was consistent with results from Western blots (data not shown).
Found at: doi:10.1371/journal.pone.0004820.s011 (1.10 MB TIF)

Acknowledgments

We are grateful to Dr. A. S. Knisely for critical review of the manuscript, Drs. K. Humphries and H. Niwa, respectively, for providing human *HOXB4* cDNA and EB3 cells, and H. Meguro for assistance in DNA microarray analysis.

Author Contributions

Conceived and designed the experiments: KM HE. Performed the experiments: KM TI TN TO. Analyzed the data: KM TI TN TO KE HA HE. Contributed reagents/materials/analysis tools: SM JiM. Wrote the paper: HN HE.

References

1. Moore MAS (2004) Ontogeny of the hematopoietic system. In: Lanza R, Gearhart J, Hogan B, Melton D, Pedersen R, et al., eds. Handbook of stem cells. Burlington: Elsevier Academic Press. pp 159–174.
2. Jaffredo T, Nottingham W, Liddiard K, Bollerot K, Pouget C, et al. (2005) From hemangioblast to hematopoietic stem cell: an endothelial connection? Exp Hematol 33: 1029–1040.
3. Kennedy M, Firpo M, Choi K, Wall C, Robertson S, et al. (1997) A common precursor for primitive erythropoiesis and definitive haematopoiesis. Nature 386: 488–493.
4. Muller AM, Medvinsky A, Strouboulis J, Grosveld F, Dzierzak E (1994) Development of hematopoietic stem cell activity in the mouse embryo. Immunity 1: 291–301.

5. Cumano A, Ferraz JC, Klaine M, Di Santo JP, Godin I (2001) Intraembryonic, but not yolk sac hematopoietic precursors, isolated before circulation, provide long-term multilineage reconstitution. Immunity 15: 477–485.
6. Yoder MC, Hiatt K, Dutt P, Mukherjee P, Bodine DM, et al. (1997) Characterization of definitive lymphohematopoietic stem cells in the day 9 murine yolk sac. Immunity 7: 335–344.
7. Lacaud G, Robertson S, Palis J, Kennedy M, Keller G (2001) Regulation of hemangioblast development. Ann N Y Acad Sci 938: 96–107; discussion 108.
8. Keller G, Kennedy M, Papayannopoulou T, Wiles MV (1993) Hematopoietic commitment during embryonic stem cell differentiation in culture. Mol Cell Biol 13: 473–486.
9. Choi K, Kennedy M, Kazarov A, Papadimitriou JC, Keller G (1998) A common precursor for hematopoietic and endothelial cells. Development 125: 725–732.
10. Nishikawa SI, Nishikawa S, Hirashima M, Matsuyoshi N, Kodama H (1998) Progressive lineage analysis by cell sorting and culture identifies FLK1+VE-cadherin+ cells at a diverging point of endothelial and hemopoietic lineages. Development 125: 1747–1757.
11. Kyba M, Perlingeiro RC, Daley GQ (2002) HoxB4 confers definitive lymphoid-myeloid engraftment potential on embryonic stem cell and yolk sac hematopoietic progenitors. Cell 109: 29–37.
12. Wang N, Satoskar A, Faubion W, Howie D, Okamoto S, et al. (2004) The cell surface receptor SLAM controls T cell and macrophage functions. J Exp Med 199: 1255–1264.
13. Lengerke C, Schmitt S, Bowman TV, Jang IH, Maouche-Chretien L, et al. (2008) BMP and Wnt specify hematopoietic fate by activation of the Cdx-Hox pathway. Cell Stem Cell 2: 72–82.
14. McKinney-Freeman SL, Lengerke C, Jang IH, Schmitt S, Wang Y, et al. (2008) Modulation of murine embryonic stem cell-derived CD41+c-kit+ hematopoietic progenitors by ectopic expression of Cdx genes. Blood 111: 4944–4953.
15. Ferkowicz MJ, Starr M, Xie X, Li W, Johnson SA, et al. (2003) CD41 expression defines the onset of primitive and definitive hematopoiesis in the murine embryo. Development 130: 4393–4403.
16. Mikkola HK, Fujiwara Y, Schlaeger TM, Traver D, Orkin SH (2003) Expression of CD41 marks the initiation of definitive hematopoiesis in the mouse embryo. Blood 101: 508–516.
17. Emambokus NR, Frampton J (2003) The glycoprotein IIb molecule is expressed on early murine hematopoietic progenitors and regulates their numbers in sites of hematopoiesis. Immunity 19: 33–45.
18. Bertrand JY, Giroux S, Golub R, Klaine M, Jalil A, et al. (2005) Characterization of purified intraembryonic hematopoietic stem cells as a tool to define their site of origin. Proc Natl Acad Sci U S A 102: 134–139.
19. Matsubara A, Iwama A, Yamazaki S, Furuta C, Hirasawa R, et al. (2005) Endomucin, a CD34-like sialomucin, marks hematopoietic stem cells throughout development. J Exp Med 202: 1483–1492.
20. Furuta C, Ema H, Takayanagi S, Ogaeri T, Okamura D, et al. (2006) Discordant developmental waves of angioblasts and hemangioblasts in the early gastrulating mouse embryo. Development 133: 2771–2779.
21. Fujimoto T, Ogawa M, Minegishi N, Yoshida H, Yokomizo T, et al. (2001) Step-wise divergence of primitive and definitive haematopoietic and endothelial cell lineages during embryonic stem cell differentiation. Genes Cells 6: 1113–1127.
22. Ito T, Tajima F, Ogawa M (2000) Developmental changes of CD34 expression by murine hematopoietic stem cells. Exp Hematol 28: 1269–1273.
23. Matsuoka S, Ebihara Y, Xu M, Ishii T, Sugiyama D, et al. (2001) CD34 expression on long-term repopulating hematopoietic stem cells changes during developmental stages. Blood 97: 419–425.
24. Sauvageau G, Thorsteinsdottir U, Eaves CJ, Lawrence HJ, Largman C, et al. (1995) Overexpression of HOXB4 in hematopoietic cells causes the selective expansion of more primitive populations in vitro and in vivo. Genes Dev 9: 1753–1765.
25. Smith RA, Glomski CA (1982) "Hemogenic endothelium" of the embryonic aorta: Does it exist? Dev Comp Immunol 6: 359–368.
26. Osawa M, Hanada K, Hamada H, Nakauchi H (1996) Long-term lymphohematopoietic reconstitution by a single CD34-low/negative hematopoietic stem cell. Science 273: 242–245.
27. Morrison SJ, Hemmati HD, Wandycz AM, Weissman IL (1995) The purification and characterization of fetal liver hematopoietic stem cells. Proc Natl Acad Sci U S A 92: 10302–10306.
28. Okada S, Nakauchi H, Nagayoshi K, Nishikawa S, Nishikawa S, et al. (1991) Enrichment and characterization of murine hematopoietic stem cells that express c-kit molecule. Blood 78: 1706–1712.
29. Keller G (2005) Embryonic stem cell differentiation: emergence of a new era in biology and medicine. Genes Dev 19: 1129–1155.
30. Nobuhisa I, Ohtsu N, Okada S, Nakagata N, Taga T (2007) Identification of a population of cells with hematopoietic stem cell properties in mouse aorta-gonad-mesonephros cultures. Exp Cell Res 313: 965–974.
31. Schiedlmeier B, Santos AC, Ribeiro A, Moncaut N, Lesinski D, et al. (2007) HOXB4's road map to stem cell expansion. Proc Natl Acad Sci U S A 104: 16952–16957.
32. Sanchez MJ, Holmes A, Miles C, Dzierzak E (1996) Characterization of the first definitive hematopoietic stem cells in the AGM and liver of the mouse embryo. Immunity 5: 513–525.
33. Kiel MJ, Yilmaz OH, Iwashita T, Yilmaz OH, Terhorst C, et al. (2005) SLAM family receptors distinguish hematopoietic stem and progenitor cells and reveal endothelial niches for stem cells. Cell 121: 1109–1121.
34. Kim I, He S, Yilmaz OH, Kiel MJ, Morrison SJ (2006) Enhanced purification of fetal liver hematopoietic stem cells using SLAM family receptors. Blood 108: 737–744.
35. Suzuki A, Andrew DP, Gonzalo JA, Fukumoto M, Spellberg J, et al. (1996) CD34-deficient mice have reduced eosinophil accumulation after allergen exposure and show a novel crossreactive 90-kD protein. Blood 87: 3550–3562.
36. Abkowitz JL, Chen J (2007) Studies of c-Mpl function distinguish the replication of hematopoietic stem cells from the expansion of differentiating clones. Blood 109: 5186–5190.
37. Takakura N, Watanabe T, Suenobu S, Yamada Y, Noda T, et al. (2000) A role for hematopoietic stem cells in promoting angiogenesis. Cell 102: 199–209.
38. Bowie MB, McKnight KD, Kent DG, McCaffrey L, Hoodless PA, et al. (2006) Hematopoietic stem cells proliferate until after birth and show a reversible phase-specific engraftment defect. J Clin Invest 116: 2808–2816.
39. Kim I, Saunders TL, Morrison SJ (2007) Sox17 dependence distinguishes the transcriptional regulation of fetal from adult hematopoietic stem cells. Cell 130: 470–483.
40. Samokhvalov IM, Samokhvalova NI, Nishikawa S (2007) Cell tracing shows the contribution of the yolk sac to adult haematopoiesis. Nature 446: 1056–1061.
41. Takahashi K, Tanabe K, Ohnuki M, Narita M, Ichisaka T, et al. (2007) Induction of pluripotent stem cells from adult human fibroblasts by defined factors. Cell 131: 861–872.
42. Yu J, Vodyanik MA, Smuga-Otto K, Antosiewicz-Bourget J, Frane JL, et al. (2007) Induced pluripotent stem cell lines derived from human somatic cells. Science 318: 1917–1920.
43. Mizoguchi H, Hayakawa T (2002) The tet-off system is more effective than the tet-on system for regulating transgene expression in a single adenovirus vector. J Gene Med 4: 240–247.
44. Miyazaki S, Miyazaki T, Tashiro F, Yamato E, Miyazaki J (2005) Development of a single-cassette system for spatiotemporal gene regulation in mice. Biochem Biophys Res Commun 338: 1083–1088.
45. Zhou S, Schuetz JD, Bunting KD, Colapietro AM, Sampath J, et al. (2001) The ABC transporter Bcrp1/ABCG2 is expressed in a wide variety of stem cells and is a molecular determinant of the side-population phenotype. Nat Med 7: 1028–1034.
46. Ema H, Takano H, Sudo K, Nakauchi H (2000) In vitro self-renewal division of hematopoietic stem cells. J Exp Med 192: 1281–1288.

Cytokine 46 (2009) 127–136

Contents lists available at ScienceDirect

Cytokine

journal homepage: www.elsevier.com/locate/issn/10434666

T cell growth control using hapten-specific antibody/interleukin-2 receptor chimera

Takahiro Sogo [a], Masahiro Kawahara [a,*], Hiroshi Ueda [a], Makoto Otsu [b], Masafumi Onodera [c], Hiromitsu Nakauchi [b], Teruyuki Nagamune [a]

[a] Department of Chemistry and Biotechnology, School of Engineering, The University of Tokyo, 7-3-1 Hongo, Bunkyo-ku, Tokyo 113-8656, Japan
[b] Division of Stem Cell Therapy, Center for Stem Cell and Regenerative Medicine, Institute of Medical Science, The University of Tokyo, 4-6-1, Shirokanedai, Minato-ku, Tokyo 108-8639, Japan
[c] Department of Genetics, National Research Institute for Child Health and Development, 2-10-1, Okura, Setagaya-ku, Tokyo 157-8535, Japan

ARTICLE INFO

Article history:
Received 9 July 2008
Received in revised form 10 December 2008
Accepted 29 December 2008

Keywords:
Chimeric receptor
Interleukin-2 receptor
Growth control
Single chain Fv
T cell

ABSTRACT

IL-2 is a cytokine that is essential for the expansion and survival of activated T cells. Although adoptive transfer of tumor-specific T cells with IL-2 is one of strategies for cancer immunotherapy, it is essential to replace IL-2 that exerts severe side effects in vivo. To solve this problem, we propose to use an antibody/IL-2R chimera, which can transduce a growth signal in response to a cognate antigen. We constructed two chimeras, in which ScFv of anti-fluorescein antibody was tethered to extracellular D2 domain of erythropoietin receptor and transmembrane/cytoplasmic domains of IL-2Rβ or γ chain. When the chimeras were co-expressed in IL-3-dependent pro-B cell line Ba/F3 and IL-2-dependent T cell line CTLL-2, gene-modified cells were selectively expanded in the absence of IL-3 and IL-2, respectively, by adding fluorescein-conjugated BSA (BSA-FL) as a cognate antigen. Growth assay revealed that the cells with the chimeras transduced a growth signal in a BSA-FL dose-dependent manner. Furthermore, STAT3, STAT5, ERK1/2 and Akt, which are hallmarks for IL-2R signaling, were all activated by the chimeras in CTLL-2 transfectant. We also demonstrated that the chimeras were functional in murine primary T cells. These results demonstrate that the antibody/IL-2R chimeras could substantially mimic the wild-type IL-2R and could specifically expand gene-modified T cells in the presence of the cognate antigen.

1. Introduction

Interleukin-2 (IL-2) is an important immunomodulatory cytokine that promotes proliferation, activation and differentiation of T cells, and is also necessary for B cell and natural killer (NK) cell function. IL-2 binds to IL-2 receptor (IL-2R) consisting of three subunits, i.e. IL-2Rα, IL-2Rβ and IL-2Rγ chains, and induces heterotrimerization of them, followed by signal transduction. IL-2Rα alone or IL-2Rβ alone has low affinity ($K_d \approx 10$ nM or ≈100 nM) to IL-2, while IL-2Rγ alone has no detectable affinity to IL-2. A high-affinity receptor ($K_d \approx 10$ pM) is composed of all three chains, whereas in the absence of IL-2Rα expression, the other two chains have intermediate affinity ($K_d \approx 1$ nM) to IL-2 [1,2]. Naïve T cells express IL-2Rγ and low levels of IL-2Rβ, but do not express IL-2Rα, resulting in less sensitivity to IL-2. The expression of IL-2Rα is restricted to activated T cells through activation of T cell antigen receptor-mediated signaling, and allows the cells to respond to IL-2 for proliferation. Although IL-2Rα is required for the high-affinity receptor complex, IL-2Rα is dispensable for signaling, since ectopic expression of either c-kit/IL-2Rβ and c-kit/IL-2Rγ chimeras or GM-CSFRα/IL-2Rγ and GM-CSFRβ/IL-2Rβ chimeras induced ligand-dependent cell proliferation of CTLL-2 T cell line [3]. These results demonstrated that a heterodimerization of IL-2Rβ and γ chains may be sufficient for transducing growth signal in T cells.

Genetic modification of T cells is an effective approach to improve anti-cancer immunotherapy and to study T cell functions. Many investigators have tried to utilize T cells for cancer immunotherapy. One promising approach is an adoptive transfer therapy, in which tumor-specific autologous T cells are isolated, expanded in vitro and reinfused with IL-2 for further expansion in vivo [4–8]. The problem is that because most tumor antigens have very low antigenicity and their expression levels are low, rapid expansion and long-lasting maintenance of a large number of tumor-specific T cells are difficult in vivo, leading to insufficient therapeutic effect. In fact, the targets of previous reports and clinical trials have been restricted to the tumors having high antigenicity like melanoma cells and viral-antigen-expressing tumors [9–11]. Therefore, expansion of transferred T cells in vivo is critical for an efficient immunotherapy. However, T cell expansion by administrating high-dose IL-2 causes undesirable side effects such as vascular leak syndrome, and cardiac and pulmonary dysfunction, because IL-2 also directly or indirectly activates several other immune cells including NK cells, B cells, neutrophils and macrophages [12,13]. One possible clue to overcome this problem is to genetically mod-

* Corresponding author. Fax: +81 3 5841 8657.
E-mail address: kawahara@bio.t.u-tokyo.ac.jp (M. Kawahara).

1043-4666/$ - see front matter © 2009 Elsevier Ltd. All rights reserved.
doi:10.1016/j.cyto.2008.12.020

ify autologous T cells with an engineered IL-2R that could respond to non-toxic substance.

We previously developed an antigen-mediated genetically modified cell amplification (AMEGA) system using an antibody/receptor chimera that triggers a growth signal in response to a specific antigen [14–16]. An anti-fluorescein single-chain Fv (ScFv) was fused to extracellular D2 domain of erythropoietin receptor (EpoR) and transmembrane and cytoplasmic domains of gp130 to create an antibody/receptor chimera (ScFvg). When IL-3-dependent murine pro-B cell line Ba/F3 was transduced with the antibody/receptor chimera, fluorescein-conjugated BSA (BSA-FL) induced oligomerization of ScFvg chains, enabling cell growth in the medium containing BSA-FL but without IL-3 [15]. In this study, we replaced the cytoplasmic domain of ScFvg with that of IL-2Rβ and γ chains to construct antibody/IL-2R chimeras that can mimic an IL-2-mediated growth signal with BSA-FL-mediated one (Fig. 1A). We investigated whether these chimeras could be functional in Ba/F3 cells, an IL-2 dependent T cell line CTLL-2 and murine primary T cells.

2. Materials and methods

2.1. Vector construction

A plasmid pBS-Eβ-IG [17] encoding a mouse IL-2Rβ chain, a plasmid pBS-I-SEγ-IG [17] encoding a mouse IL-2Rγ chain, and a retroviral vector pMK-ScFvg [18] encoding anti-FL ScFv clone 31IJ3, were used as starting constructs. pBS-Eβ-IG was digested with BspEI and NotI, and inserted into pMK-ScFvg digested with the same enzymes to make pMK-SEβ-IG. NcoI-digested pMX-ScFvgIGFP [15] was inserted into NcoI-digested pBS-ILgIGFP [19], resulting in pBS-I-Sg-IG. BspEI-NotI-digested pBS-I-LEγ-IG was subcloned into pBS-I-Sg-IG digested with the same enzymes to create pBS-I-SEγ-IG. Then pBS-I-SEγ-IG was digested with AvrII and inserted into AvrII-digested pMK-SEβ-IG, resulting in pMK-SβISγ-IG.

pGCDNsam-based retroviral expression vectors were constructed for producing retrovirus pseudotyped with a vesicular stomatitis virus G protein (VSV-G) [40,41]. pMK-SEβ-IG and pMK-SEγ-IG were digested with BspEI and BamHI and inserted into pGCDNsam-SEmpI-IG and pGCDNsam-SEmpI-IK (manuscript in preparation) digested with the same enzymes resulting in pGCDNsam-Sβ-IG and pGCDNsam-Sγ-IK, respectively. In pGCDNsam-Sβ-IG and pGCDNsam-Sγ-IK, the genes encoding chimeric Sβ chain and Sγ chain were individually inserted into upstream of IRES-EGFP and IRES-Kusabira Orange (KO) [42], respectively (Fig. 7A).

2.2. Ligand preparation

Bovine serum albumin–fluorescein isothiocyanate conjugate (BSA-FL) was purchased from Sigma (St. Louis, MO). Fluorescein dimer was prepared as described previously [15]. The sequences of

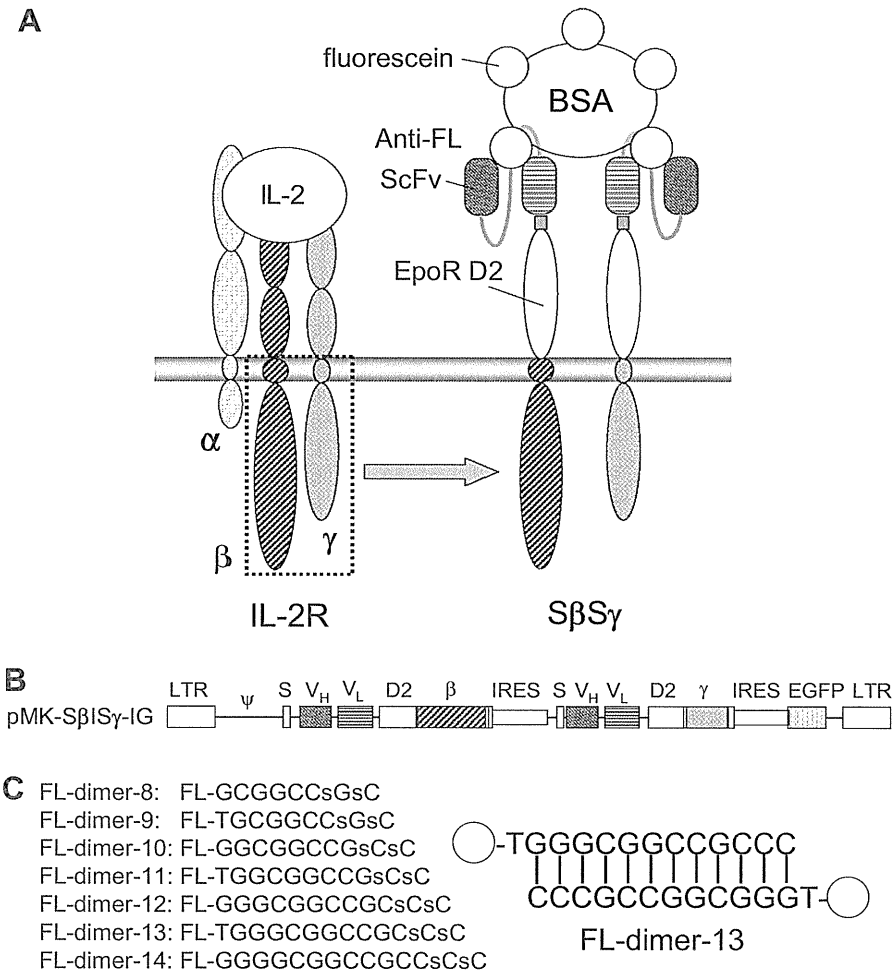

Fig. 1. The constructs of chimeric receptor and FL-dimers. (A) The schematic illustration of wild-type and chimeric IL-2R. (B) The construction of chimeric IL-2R vector. A retroviral vector with long terminal repeats (LTRs) and a packaging signal (Ψ) was used. An immunoglobulin heavy chain secretion signal sequence (S) is placed upstream of the chimeric receptor genes for cell surface expression. (C) The constructs of FL-dimers. Several lengths of fluorescein-conjugated palindromic DNAs (8–14 mer) were self-annealed to make FL-dimers. The illustration of FL-dimer-13 is shown as a representative.

the palindromic DNA linkers were as follows: 8 mer, FL-GCGG CCsGsC; 9 mer, FL-TGCGGCCsGsC; 10 mer, FL-GGCGGCCGsCsC; 11 mer, FL-TGGCGGCCGsCsC; 12 mer, FL-GGGCGGCCGCsCsC; 13 mer, FL-TGGGCGGCCGCsCsC; 14 mer, FL-GGGGCGGCCGCCsCsC. The 3′-terminal two bases in each FL-labeled DNA were made with s-oligo to prevent degradation by exonucleases. These FL-labeled s-oligo DNAs were purchased from Proligo (La Jolla, CA).

2.3. Cell culture

A murine IL-3-dependent pro-B cell line, Ba/F3 [20] was cultured in RPMI 1640 medium (Nissui Pharmaceutical, Tokyo, Japan) supplemented with 10% FBS (Biowest, Paris, France) and 1 ng/ml murine IL-3 (R&D systems, Cambridge, MA). A murine IL-2-dependent T cell line, CTLL-2 [21] was cultured in RPMI 1640 medium supplemented with 10% FBS, 2 ng/ml murine IL-2 (R&D systems), 1 mM sodium pyruvate, 50 μM monothioglycerol and 20 nM bathocuproine disulfonate (Sigma) [22]. We used three retroviral packaging cell lines. Plat-E [23] was cultured in Dulbecco's modified Eagle's medium (DMEM) (Nissui Pharmaceutical) supplemented with 10% FBS, 1 μg/ml puromycin (Sigma) and 10 μg/ml blasticidin (Kaken Pharmaceutical, Tokyo, Japan). 293GP was cultured in DMEM with 10% FBS. 293GPG was cultured in DMEM with 10% FBS, 2 μg/ml puromycin, 300 μg/ml G418 (Calbiochem, Darmstadt, Germany) and 1 μg/ml tetracycline (Sigma).

2.4. Vector transduction/transfection of Ba/F3 and CTLL-2

Ba/F3 cells were retrovirally transduced, as previously described [15]. In brief, Plat-E cells were transfected with the retroviral vector pMK-SβISγ-IG by lipofection and the culture medium was used as a viral supernatant. Ba/F3 cells were transduced with the viral supernatant in the presence of 10 μg/ml polybrene (Sigma) and 2 ng/ml IL-3 in a 24-well plate, and the transduced cells were designated as Ba/SβSγ. CTLL-2 cells were transfected with SspI-digested linear pMK-SβISγ-IG plasmid (20 μg) and pMXs-neo plasmid (1 μg) by electroporation in the presence of 100 μM spermine (Sigma). The cells (3×10^6 in 500 μl of RPMI medium) mixed with the vectors were transferred to a 4 mm-gap cuvette, and electroporation was performed at 300 V and 1000 μF using an Electroporator II (Invitrogen, Groningen, The Netherlands). Subsequently, transfected cells were inoculated into a 100 mm diameter dish and cultured in a 5% CO_2 incubator at 37 °C. Transfected cells were designated as CT/SβSγ.

2.5. Retroviral transduction of murine primary T cells

A retroviral packaging cell line, 293GP was co-transfected with pGCDNsam expression vector and pcDNA3.1-VSV-G vector encoding VSV-G envelope gene by lipofection for a transient production of VSV-G pseudotyped retroviruses. Culture medium of transfected 293GP was collected and subsequently used for transduction of 293GPG that had been engineered to express the VSV-G protein under control of a tetracycline-inducible system [40]. 293GPG cells transduced with pGCDNsam-Sβ-IG or pGCDNsam-Sγ-IK stably produced retroviruses encoding the respective genes. The culture supernatant of transduced 293GPG was collected and centrifuged at 6000*g* for 16 h at 4 °C, followed by resuspension of viral pellet in StemPro-34 SFM (Invitrogen) to obtain 100-fold concentrated virus.

To isolate mouse primary T cells, splenocytes were harvested from 10 weeks old male C57BL/6 mice (Japan SLC, Shizuoka, Japan) and labeled with anti-CD90.2 microbeads (Miltenyi, Auburn, CA), followed by magnetic cell sorting. Isolated CD90.2 positive T cells were subsequently inoculated into a 24-well plate (2×10^6 cells/well) in RPMI1640 medium supplemented with 10% FBS, 5 μM 2-mercaptoethanol, 10 ng/ml IL-2, and 20 μl Dynabeads mouse CD3/CD28 T cell expander (Invitrogen). The T cells cultured for 24 h were then seeded into a 24-well plate coated with retronectin (Takara, Shiga, Japan) with 15 μl each of Sβ-IG and Sγ-IK viral supernatants ($1–2 \times 10^8$ transducing units/ml for Jurkat cells), and incubated for 24 h in RPMI1640 with 2% FBS and 10 ng/ml IL-2. The cells were also co-transduced with two mock vectors encoding IG alone and IK alone as a negative control. After another 24 h culture in RPMI1640 with 10% FBS and 10 ng/ml IL-2, transduction efficiency of the cells were analyzed by flow cytometry.

2.6. Selection of the transfectants/transductants and cell proliferation assay

For selection of the Ba/SβSγ and CT/SβSγ, the cells were washed with PBS and inoculated into 24-well plates. Ba/SβSγ was selected in the medium containing either no factor, 5 μg/ml BSA-FL, or 1 ng/ml IL-3. CT/SβSγ was initially selected in the medium containing 2 ng/ml IL-2 and 800 μg/ml G418, followed by selection in the medium with 5 μg/ml BSA-FL. For cell proliferation assay, the selected cells were washed with PBS and were seeded into 24-well plates at 10^4 or 5×10^4 cells/ml with indicated concentrations of each ligand. The viable cell numbers were counted by a hemocytometer and trypan blue exclusion assay.

Murine primary T cells transduced with mock vectors (IG and IK), Sβ-IG alone, Sγ-IK alone and both Sβ-IG and Sγ-IK were sorted using MoFlo fluorescence-activated cell sorter (Dako, Glostrup, Denmark) and cultured with 10 ng/ml IL-2 for two days. The cells were washed twice with PBS containing 2% FBS to remove IL-2, and subsequently inoculated into a 48-well plate at 1.5×10^5 cells/well with no ligand, 5 μg/ml BSA-FL, or 10 ng/ml IL-2 and cultured for three days. Viable cells were determined as propidium iodide (PI)-negative cells and their numbers were counted by flow cytometric analysis using Flow-Count (Beckman Coulter, Fullerton, CA).

2.7. Western blotting

The cells (10^6 cells) were washed with PBS, lysed with 100 μl of lysis buffer (20 mM Hepes, 150 mM NaCl, 10% glycerol, 1% Triton X-100, 1.5 mM $MgCl_2$, 1 mM EGTA, 10 μg/ml aprotinin, 10 μg/ml leupeptin, pH 7.5) and incubated on ice for 10 min. After centrifugation at 16,000*g* for 10 min, the supernatant was mixed with Laemmli's sample buffer and boiled. The lysate was resolved by SDS–PAGE and transferred to a nitrocellulose membrane (Millipore, Bedford, MA). After the membrane was blocked with 5% skimmed milk or 1% BSA, the blot was probed with appropriate dilutions of primary and secondary antibodies, and detection was performed using Chemi-Lumi One (Nacalai tesque, Kyoto, Japan). The primary rabbit antibodies anti-human IL-2Rβ, anti-human IL-2Rγ, anti-mouse STAT3, anti-mouse STAT5 and anti-mouse ERK1/2 were from Santa Cruz Biotechnology (Santa Cruz, CA), anti-phospho-ERK1/2 was from Promega (Madison, WI), anti-phospho-STAT3, anti-phospho-STAT5, anti-Akt and anti-phospho-Akt were from Cell Signaling Technology (Danvers, MA). HRP-conjugated anti-rabbit IgG was from Biosource (Camarillo, CA).

2.8. Flow cytometric analysis

Ba/SβSγ and CT/SβSγ were washed once with PBS and resuspended with RPMI 1640, whereas primary T cell-transductants were washed twice with PBS containing 2% FBS and resuspended with PBS containing 2% FBS. Fluorescence intensities of EGFP, KO and PI were measured using a FACSCalibur flow cytometer (Becton Dickinson, Lexington, KY) at 488 nm excitation and fluorescence detection at 530 ± 15 nm, 585 ± 21 nm and >650 nm, respectively. Cell sorting

of transduced primary T cells was performed by MoFlo flow cytometer using fluorescence intensities of EGFP and KO as indicators.

2.9. Starvation and stimulation of cells

Cells were washed twice with PBS and starved in the depletion medium (RPMI 1640, 10% FBS) for 12 h. Cells (5×10^6–1×10^7) were stimulated with 2 ml medium containing various ligands at 37 °C. Ba/F3 and its transductants were stimulated with 1 ng/ml IL-3, 5 μg/ml BSA-FL or 0.5 μM FL-dimer (13 mer), and CTLL-2 and its transfectants were stimulated with 2 ng/ml IL-2, 5 μg/ml BSA-FL or 0.5 μM FL-dimer (13 mer). After 10- or 15-min incubation, the cells were added with 2 ml of 2 mM ice-cold Na_3VO_4 in PBS, pelleted and lysed with 100 μl/10^6 cells of lysis buffer to prepare lysates for Western blot analysis.

3. Results

3.1. Selective expansion of genetically modified cells by BSA-FL

We designed an antibody/IL-2R chimera (SβSγ) that can selectively transduce an IL-2-mediated growth signal in genetically modified cells (Fig. 1A and B). The SβSγ chimera can recognize a pair of fluorescein molecules as a cognate ligand. Besides Sβ and Sγ genes, EGFP gene was inserted in pMK-SβISγ-IG vector to facilitate identification of gene-modified cells. Previous reports described that heterologous expression of chimeric IL-2Rs in an IL-3-dependent murine pro-B cell line Ba/F3 and in an IL-2-dependent murine T cell line CTLL-2 was sufficient for their proliferation in response to cognate ligands [3]. Thus, we performed functional analysis of SβSγ chimera by using Ba/F3 and CTLL-2 cells.

Ba/F3 cells were retrovirally transduced with pMK-SβISγ-IG, whereas CTLL-2 cells, which were hardly transducible by retrovirus (data not shown), were transfected with the same vector by using electroporation. For selection of the transductant/transfectant, we used BSA-FL as a ligand, because multiple fluorescein molecules in BSA-FL would facilitate oligomerization of the chimera. Ba/F3 transductant was selected in the media with 5 μg/ml BSA-FL or 1 ng/ml IL-3 for 26 or 31 days, respectively, followed by flow cytometric analysis to examine EGFP-positive cell ratios. The EGFP-positive cell ratio of BSA-FL-selected cells was almost 100%, while those of IL-3-selected cells were similar to those before selection (Fig. 2A). As for CTLL-2 transfectant, although we first attempted selection directly in the media with BSA-FL, all the cells underwent apoptotic cell death. As it might be partly due to very low frequency of transfected cells (about 0.05%) before selection, CTLL-2 cells were co-transfected with G418-resistant gene as well as pMK-SβISγ-IG, followed by selection with 800 μg/ml G418 in the presence of IL-2 in order to increase the population of transfected cells. Consequently, almost all of the cells were EGFP-positive after 18-day culture with G418 (Fig. 2B). When these cells were subsequently cultured in the medium with 5 μg/ml BSA-FL in the absence of IL-2 and G418, they successfully grew in response to BSA-FL and selected cells were all EGFP-positive after 29-day culture (Fig. 2B). Resultant selected Ba/F3 and CTLL-2 cells were designated as Ba/SβSγ and CT/SβSγ, respectively.

To investigate whether cell proliferation during BSA-FL selection was induced by the expressed chimeric IL-2Rs, the amounts of expressed chimeric receptors were compared by Western blotting. BSA-FL-selected transfectants/transductants exclusively showed distinct bands of Sβ and Sγ migrated around 72 kDa and 52 kDa, respectively (Fig. 3A and B). These results indicate that only the cells expressing the SβSγ chimera can grow in response to BSA-FL, leading to successful mimicry of an IL-2 signal in Ba/F3 and CTLL-2 cells.

3.2. BSA-FL dose-dependent cell growth of the transfectants/transductants

We next performed cell proliferation assay to evaluate whether the growth of selected cells is promoted in a BSA-FL dose-dependent manner. When Ba/SβSγ and CT/SβSγ were cultured in the media containing various concentrations of BSA-FL, both cells showed BSA-FL dose-dependent cell proliferation (Fig. 4). The lower limits for BSA-FL-dependent cell growth were between 0.1 and 1 μg/ml for both Ba/SβSγ and CT/SβSγ, and BSA-FL concentration below 0.1 μg/ml did not induce any cell growth during the culture period tested. Therefore, SβSγ chimera could promote proliferation of genetically modified cells in a BSA-FL-dependent manner without any apparent background cell growth.

3.3. Cell growth control using dimerized fluorescein

Since BSA-FL contains an immunogenic carrier protein BSA and the distances between the fluorescein molecules are unclear, we previously designed a series of dimerized fluorescein (FL-dimers) tethered with a palindromic oligo-DNA linker [15]. The lengths and sequences of the oligo-DNA linkers for FL-dimers are shown in Fig. 1C. First we cultured Ba/SβSγ and CT/SβSγ cells with various lengths of FL-dimers ranging from FL-dimer-8 (27.2 Å) to FL-dimer-14 (47.6 Å). Ba/SβSγ cells were cultured with 1 μM of each FL-dimer for 3 days, while CT/SβSγ cells were cultured with 0.5 μM of each FL-dimer for 4 days, followed by counting the viable cell number. Consequently, the optimal length of FL-dimer was FL-dimer-12 or FL-dimer-13 for Ba/SβSγ cells and FL-dimer-13 for CT/SβSγ cells. Interestingly, both cells could hardly grow in the presence of FL-dimers-8, -9, -10 and -14 (Fig. 5A and B). Compared with our previous report of a gp130 chimera, the growth activity via the SβSγ chimera is highly dependent on the length of FL-dimer, whereas the optimal linker length was similar [15]. To investigate FL-dimer dose-dependency for cell growth, Ba/SβSγ and CT/SβSγ were cultured with various concentrations of FL-dimer-13. Both Ba/SβSγ and CT/SβSγ cells showed maximum cell proliferation at 0.5 μM, and there was no apparent difference between these two cell lines (Fig. 5C and D). The optimal concentration of the FL-dimer is consistent with the previous report of the gp130 chimera as well as growth-inhibitory effect observed at higher concentrations. These results suggest that the SβSγ chimera can be properly dimerized and activated by FL-dimer.

3.4. Activation of signaling molecules via chimeric IL-2R in response to fluorescein

Heterodimerization of IL-2Rβ/IL-2Rγ subunits triggers downstream signaling events that involve the phosphorylation of various cellular proteins. IL-2 signaling activates Jak/STAT, Ras/MAPK and PI3K/Akt pathways through cellular protein kinases [24,25]. Activated Jak1 and Jak3 are able to phosphorylate signal transducer and activator of transcription (STAT) 1, STAT3 and STAT5 molecules. Phosphorylation of STAT molecules induces their dimerization, resulting in their translocation to the nucleus, where they regulate gene transcriptions. IL-2 signaling also induces tyrosine phosphorylation of IL-2Rβ, resulting in the recruitment of Shc and Grb2, followed by the activation of Ras/MAPK pathway. Syk, which is an upstream regulator of PI3K/Akt pathway, is directly associated with IL-2Rβ and is also activated by IL-2 signaling, resulting in activation of Akt [26]. To examine whether the chimeric IL-2Rs could mimic IL-2 signaling or not, phosphorylation status of STAT3, STAT5, ERK1/2 and Akt was examined by Western blotting (Fig. 6).

When CT/SβSγ was stimulated with BSA-FL or FL-dimer-13, all signal transducers tested were phosphorylated like that stimulated

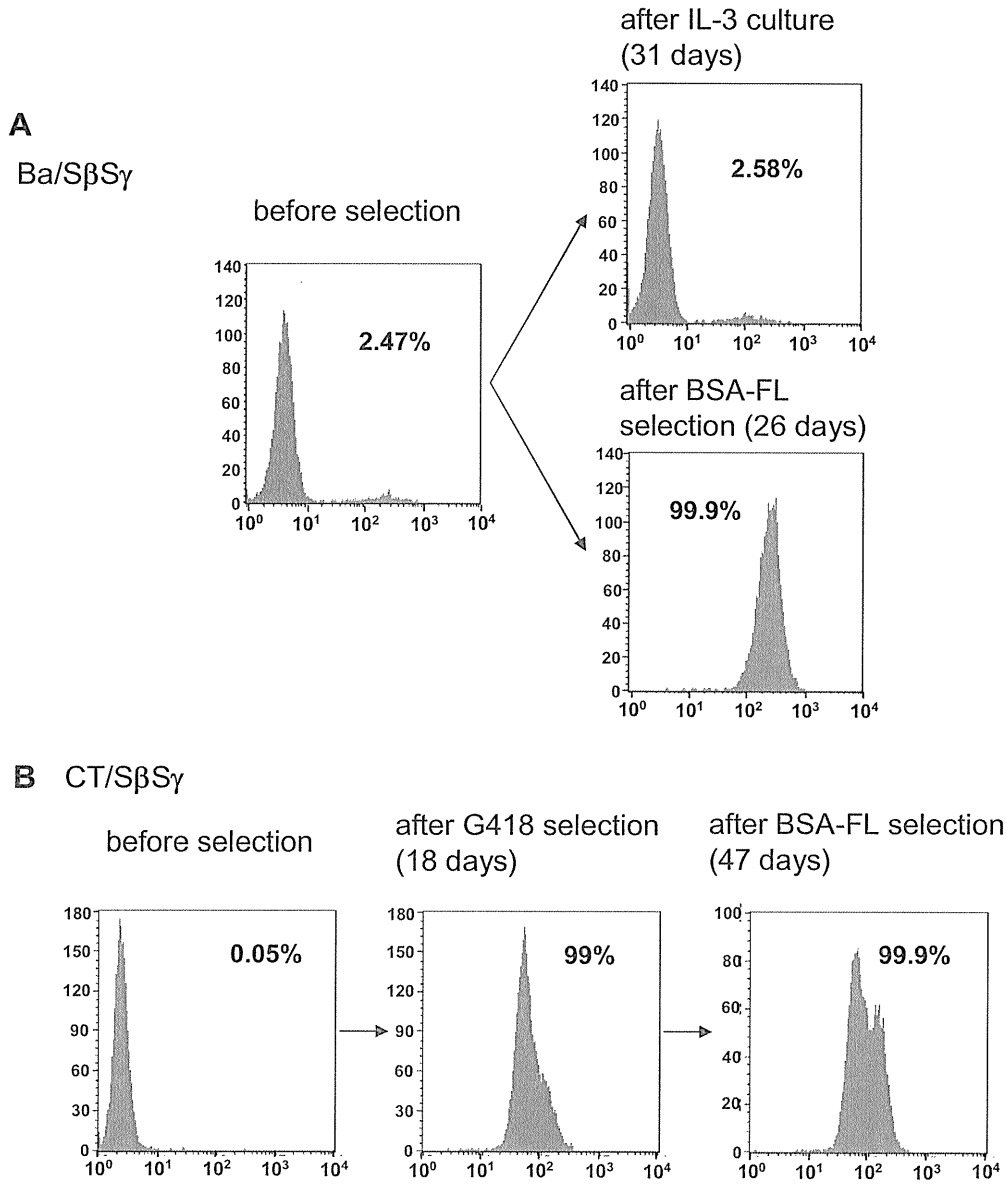

Fig. 2. Selective expansion of EGFP-positive cells with the SβSγ chimera. (A) Ba/SβSγ cells after selection with IL-3 or BSA-FL were analyzed by flow cytometry. (B) CT/SβSγ cells were selected with G418, and subsequently with BSA-FL. Cell number was plotted against log green fluorescence intensity. EGFP-negative and EGFP-positive regions were determined by taking parental Ba/F3 (A) or CTLL-2 cells (B) as a negative control. The days from gene transfer and the EGFP-positive cell ratios are indicated.

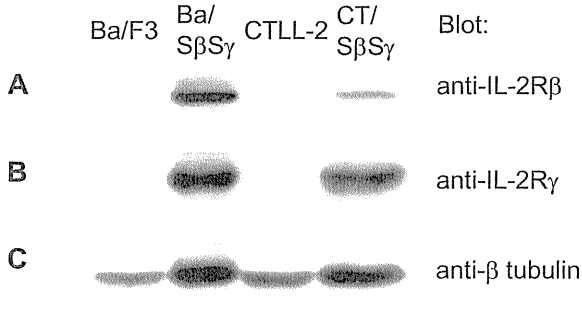

Fig. 3. Western blot analysis to confirm the expression of Sβ and Sγ chimeras in BSA-FL-selected transfectants/transductants. The expressions of chimeric IL-2Rβ (A) and IL-2Rγ (B) were detected with anti-IL-2Rβ and anti-IL-2Rγ antibodies, respectively. The expression of β-tubulin (C) was detected with anti-β tubulin antibody as a loading control.

with IL-2 (Fig. 6B), while only STAT5 and ERK1/2 were phosphorylated in BSA-FL- and FL-dimer-13-stimulated Ba/SβSγ (Fig. 6A). Based on the results of growth assay showing that Ba/SβSγ could proliferate in an antigen-dose-dependent manner (Fig. 4A and 5C), activations of STAT5 and ERK1/2 are likely to be sufficient for the growth of Ba/F3 transductant. Meanwhile, considering about the cell growth control, both Ba/SβSγ and CT/SβSγ showed strictly antigen-dose-dependent growth without any background cell growth, although STAT5 and ERK1/2 were slightly phosphorylated and Akt was constitutively activated in nonstimulated CT/SβSγ. The hyperactivations of these molecules may contribute to the subtle growth of CT/SβSγ cultured with 0.1 μg/ml BSA-FL or 0.01 μM FL-dimer-13, which was not observed in Ba/SβSγ (Fig. 4 and 5C and D). However, these hyperactivations were not strong enough for CT/SβSγ to grow without any ligand. Therefore, the SβSγ chimera can successfully control the proliferation of Ba/F3 and CTLL-2 through transducing an IL-2-like growth signal in response to the specific antigen.